

DIFFUSIVE BOLTZMANN EQUATION, ITS FLUID DYNAMICS, COUETTE FLOW AND KNUDSEN LAYERS

RAFAIL V. ABRAMOV

ABSTRACT. In the current work we propose a diffusive modification of the Boltzmann equation. This modification naturally leads to the corresponding diffusive fluid dynamics equations, which we numerically investigate in a simple Couette flow setting. This diffusive modification is based on the assumption of the “imperfect” model collision term, which is unable to track all collisions in the corresponding real gas particle system, due to the fact that some of the collisions are induced by effects the Boltzmann collision operator is “unaware of”. The effect of missed collisions is then modeled by an empirically scaled long-term stochastic homogenization process of the particle dynamics, which equips the corresponding Boltzmann equation with a spatial diffusion term. The corresponding diffusive fluid dynamics equations are then obtained in a standard way by closing the hierarchy of the moment equations using either the Euler, Navier-Stokes, Grad, or regularized Grad closure. In the numerical experiments with the Couette flow, we discover that the full-fledged Knudsen velocity boundary layers develop with all tested closures when the viscosity and diffusivity are reduced in the vicinity of the walls. Additionally, we find that the component of the heat flux parallel to the direction of the flow is comparable in magnitude to its transversal component, and that the Grad closures approximate the former with good precision. We compare the simulations with the corresponding Direct Simulation Monte Carlo (DSMC) results. Argon and nitrogen are studied as examples.

1. INTRODUCTION

In the kinetic theory, the processes in gases are described by the Boltzmann equation [9–12], which models the evolution of the density $f(t, \mathbf{x}, \mathbf{v})$ of a probability distribution of a single gas particle in the space of coordinate \mathbf{x} and velocity \mathbf{v} at time t , under the assumption that all gas particles are independently and identically distributed, and that no more than two particles collide at once. The Boltzmann equation is given by

$$(1.1) \quad \frac{\partial f}{\partial t} + \mathbf{v} \cdot \nabla_{\mathbf{x}} f = \mathcal{C}(f),$$

where $\mathcal{C}(f)$ is the collision term (also called the collision operator [20, 26]), specified by

$$(1.2) \quad \mathcal{C}(f) = \int B(\mathbf{v}_2 - \mathbf{v}, \boldsymbol{\omega}) (f(\mathbf{v}')f(\mathbf{v}'_2) - f(\mathbf{v})f(\mathbf{v}_2)) d\boldsymbol{\omega} d\mathbf{v}_2.$$

DEPARTMENT OF MATHEMATICS, STATISTICS AND COMPUTER SCIENCE, UNIVERSITY OF ILLINOIS AT CHICAGO, 851 S. MORGAN ST., CHICAGO, IL 60607

E-mail address: abramov@math.uic.edu.

Key words and phrases. Boltzmann equation; fluid dynamics; Couette flow; Knudsen layers.

Above, ω is a unit vector, integrated over a sphere, $B \sim |(v_2 - v) \cdot \omega|$ is the collision kernel, and v' , v'_2 are defined by the energy and momentum conservation relations

$$(1.3) \quad v' = v - (\omega \cdot (v - v_2))\omega, \quad v'_2 = v_2 + (\omega \cdot (v - v_2))\omega.$$

Integrating the Boltzmann equation over various powers of the velocity variable yields the hierarchy of the fluid dynamics equations (also called the moment equations in kinetic theory), of which the lowest-order closure is provided by the well known Euler equations [4], while the next-order closure is given by the Grad equations [21, 22].

The Boltzmann equation and its corresponding hierarchy of the moment fluid dynamics equations are of the first order in space, which makes them poorly suitable for the Dirichlet boundary value problems. However, the Dirichlet boundary conditions are rather ubiquitous in the applied problems for realistic flows (for example, the Couette and Poiseuille flows). For the fluid dynamics equations, the second order in space is usually achieved via the Chapman-Enskog perturbation expansion [13, 20, 26], which, when applied to the Euler closure, leads to the famous Navier-Stokes equations [4], for which the Dirichlet boundary conditions are well posed.

Recently, there appeared a number of works on the extended fluid dynamics [6–8, 14, 15, 17], where the additional spatial diffusion was introduced into the conventional fluid dynamics equations. Some of them [6–8] were based on the idea of introducing the concept of the “volume velocity”, which differs from the usual mass velocity by a small flux term based upon Fick’s law. Others [15, 17] introduced similar additional terms to model the self-diffusion of mass. Among those listed above, the work [14] appears to employ the closest conceptual approach to what we suggest here, namely, in [14] an *ad hoc* diffusion term was introduced directly into the Boltzmann equation (1.1) via the assumption of an empirical stochasticity of particle motion, in addition to the already present inter-particle collisions.

However, the main conceptual drawback of such an approach is its seeming lack of a fundamental justification. In particular, it was noted in [14] that there was no thermodynamically justified reason to introduce an additional diffusion term into a continuum gas model. Clearly, if the assumptions on the statistical properties of collisions in (1.1) and (1.2) indeed hold, then there is certainly no reason for a spatial diffusion term, which is introduced in addition to the collision operator, to exist at all.

From what seems to us at present, the only possible justification for the existence of such a diffusion term is that the collision operator in (1.2) alone by itself is too idealized for a practical situation. Indeed, it is a fact that the velocity and temperature of a gas near a wall are usually roughly equal to those of the wall. Moreover, if a gas is placed between two walls with different velocities and temperatures, it tends to accommodate these boundary conditions at both walls at the same time, with a smooth transition in between. The fact that, in such a situation, the Boltzmann equation in (1.1) with the collision operator in (1.2) becomes overdetermined, merely signifies the deficiency of the latter.

In the current work, we introduce diffusion into the Boltzmann equation and its resulting hierarchy of the fluid dynamics equations by assuming that a particle collision model does not track all collisions of the real gas particles, and misses some of them. We

motivate such an assumption by pointing out that the collision operator of the form (1.2) is not realistic enough to be strictly valid for an actual gas (e.g. the operator does not have a provision to describe the collisions of the gas molecules with the molecules of a nearby wall). We then propose to model the effect of the missed collisions via the appropriately scaled centered homogenization dynamics of the model, which is, in turn, obtained from the underlying particle dynamics process via the appropriate multiscale expansion formalism. To derive the long-term homogenization process, a random jump model is used to parameterize the particle collision dynamics. We also ensure that the random jump model is consistent with the Boltzmann equation; that is, the Boltzmann equation can be derived from the random jump model under appropriate assumptions.

The manuscript is organized as follows. In Section 2 we start by modeling the particle collision process by a random jump process, and find that it can be reduced to the Boltzmann equation under appropriate assumptions. This allows us to work with the random jump process in order to determine the long-term behavior of the particle system in the homogenization limit, which we do in Section 3. We then assume that a model of the particle process does not track all collisions of the real particles. Under this assumption, in Section 4 we model the effect of missed collisions by introducing the appropriately scaled long-term homogenization effect into the model of particle dynamics. We then show that the resulting Boltzmann equation acquires a spatial diffusion term, which corresponds to the diffusion of mass. In Section 5 we derive the diffusive Euler, Navier-Stokes, Grad [21, 22] and regularized Grad [33, 34, 36] equations, which also inherit the spatial diffusion terms, and thus do not become overdetermined in the Dirichlet boundary value problems, unlike the conventional Euler and Grad equations. We then carry out the numerical simulations for argon and nitrogen in the simple Couette flow setting, and find that the diffusive Euler equations exhibit the behavior which is similar to both the conventional and diffusive Navier-Stokes equations. We also discover that if the viscosity and diffusivity are reduced in the vicinity of the walls, then all studied moment closures develop the full-fledged Knudsen velocity boundary layers. We find that there is a substantial component of the heat flux parallel to the direction of the flow, which the Fourier law approximation of the Navier-Stokes equations fails to capture. On the other hand, both the diffusive and regularized diffusive Grad closures approximate the parallel heat flux with good precision. To verify the results, we also carry out the Direct Simulation Monte Carlo (DSMC) computations with the same set-up. The numerical simulations are described in Sections 6 and 7. The summary is given in Section 8.

2. THE BOLTZMANN EQUATION FROM A RANDOM JUMP PROCESS

In this section we consider a system of K identical particles, which move in an N -dimensional Euclidean space. In order to define such a dynamical system in a concise manner, we concatenate all coordinates \mathbf{x}_k and velocities \mathbf{v}_k of the individual particles into the two vectors \mathbf{X} and \mathbf{V} as follows:

$$(2.1) \quad \mathbf{X} = (\mathbf{x}_1, \mathbf{x}_2, \dots, \mathbf{x}_K), \quad \mathbf{V} = (\mathbf{v}_1, \mathbf{v}_2, \dots, \mathbf{v}_K).$$

Apparently, \mathbf{X} and \mathbf{V} have the dimension KN , since each \mathbf{x}_k or \mathbf{v}_k is N -dimensional. In what follows, we will assume that the particle system (\mathbf{X}, \mathbf{V}) preserves the momentum

(the sum of all v_k) and energy (the sum of all $\|v_k\|^2$). Thus, V lives on a sphere of constant momentum and energy. The momentum and energy conservation assumptions are needed strictly to derive the Boltzmann equation in (1.1); in a realistic situation this is not necessarily the case, since, for example, heated and moving walls tend to communicate their momentum and energy to the nearby gas. In addition, for convenience we will assume that the Euclidean space of X is a torus, so that, on one hand, it does not have boundaries and particles can only collide between themselves, and, on the other hand, the particles cannot eventually escape indefinitely far from each other.

In the standard technique used for the derivation of the Boltzmann equation, the time-derivative of the multi-particle velocity process V is set to zero, and the inter-particle collisions are parameterized by defining the spatial domain in a specific way, and prescribing the appropriate boundary conditions. More details on this topic can be found in [9–12]. However, from the dynamical systems perspective, it is more preferable to work with a system where the particle interactions are incorporated directly into the “vector field” of the dynamics equations. In particular, the multiscale expansion formalism of such a system can be carried out in a standard way (see, for example, [3, 24, 31, 37]). In what follows, we demonstrate that a system where the particle interactions are parameterized through a random jump process, also reduces to the Boltzmann equation (1.1) under appropriate assumptions, and in this sense is “equivalent” to the system governed by the conventional collision process via the boundary conditions.

Here we model the velocity-collision dynamics via a random jump process as

$$(2.2) \quad \frac{dX}{dt} = V, \quad dV = dN(t),$$

where $N(t)$ is a Poisson-type Feller semigroup [1, 2], which lives on the sphere of constant momentum and energy. Thus, for a suitable function $g = g(X, V)$ we have

$$(2.3) \quad \frac{\partial}{\partial t} \mathbb{E}g = \mathcal{L}g = V \cdot \nabla_X g + \mathcal{L}_V g,$$

where $\mathbb{E}g$ is the expectation of g over the probability space of the jump process $N(t)$, \mathcal{L} is the full generator of the (X, V) -process in (2.2), and \mathcal{L}_V is the generator of the velocity process V alone.

By the Lévy-Khinchin theorem [1, 19], the generator \mathcal{L}_V has the form

$$(2.4) \quad \mathcal{L}_V g = \int (g(X + X', V + V') - g(X, V)) d\Pi_{X,V}(X', V').$$

Above, X and V are the coordinate and velocity before the jump, $X + X'$ and $V + V'$ are the same quantities after the jump, and therefore, X' and V' are the jumps themselves. The quantity Π is the Lévy measure of $N(t)$. Here we are at freedom to prescribe Π however appropriate, and we will do so to ensure the compatibility of the random jump model in (2.2) with the Boltzmann equation in (1.1). Above, the formally introduced quantity X' denotes the jumps in coordinates X , which in reality never occur, and which we account for below. The full generator \mathcal{L} , acting on the process (X, V) , is, therefore,

given by

$$(2.5) \quad \mathcal{L}g = \mathbf{V} \cdot \nabla_{\mathbf{X}} g + \int (g(\mathbf{X} + \mathbf{X}', \mathbf{V} + \mathbf{V}') - g(\mathbf{X}, \mathbf{V})) d\Pi_{\mathbf{X}, \mathbf{V}}(\mathbf{X}', \mathbf{V}').$$

Now our goal is to derive the corresponding forward Kolmogorov equation (also known as the Fokker-Planck equation [32]). Let us assume that the distribution of (\mathbf{X}, \mathbf{V}) -states is continuous with the density F , and that $d\Pi_{\mathbf{X}, \mathbf{V}}(\mathbf{X}', \mathbf{V}') = \pi(\mathbf{X}, \mathbf{V}, \mathbf{X}', \mathbf{V}') d\mathbf{X}' d\mathbf{V}'$ (where π can be singular, of course). Then, integrating against $F d\mathbf{X} d\mathbf{V}$, we obtain

$$(2.6) \quad \frac{\partial}{\partial t} \int g F d\mathbf{X} d\mathbf{V} = \int F \mathbf{V} \cdot \nabla_{\mathbf{X}} g d\mathbf{X} d\mathbf{V} + \int (g(\mathbf{X} + \mathbf{X}', \mathbf{V} + \mathbf{V}') - g(\mathbf{X}, \mathbf{V})) F(\mathbf{X}, \mathbf{V}) \pi(\mathbf{X}, \mathbf{V}, \mathbf{X}', \mathbf{V}') d\mathbf{X}' d\mathbf{V}' d\mathbf{X} d\mathbf{V}.$$

The first term in the right-hand side above is easily integrated by parts:

$$(2.7) \quad \int F \mathbf{V} \cdot \nabla_{\mathbf{X}} g d\mathbf{X} d\mathbf{V} = - \int g \mathbf{V} \cdot \nabla_{\mathbf{X}} F d\mathbf{X} d\mathbf{V}.$$

For the second term in the right-hand side of (2.6) we first use

$$(2.8) \quad \begin{aligned} \int g(\mathbf{X} + \mathbf{X}', \mathbf{V} + \mathbf{V}') F(\mathbf{X}, \mathbf{V}) \pi(\mathbf{X}, \mathbf{V}, \mathbf{X}', \mathbf{V}') d\mathbf{X}' d\mathbf{V}' d\mathbf{X} d\mathbf{V} &= \\ &= \int g(\mathbf{X}'', \mathbf{V}'') F(\mathbf{X}, \mathbf{V}) \pi(\mathbf{X}, \mathbf{V}, \mathbf{X}'' - \mathbf{X}, \mathbf{V}'' - \mathbf{V}) d\mathbf{X}'' d\mathbf{V}'' d\mathbf{X} d\mathbf{V} = \\ &= \int g(\mathbf{X}, \mathbf{V}) F(\mathbf{X}', \mathbf{V}') \pi(\mathbf{X}', \mathbf{V}', \mathbf{X} - \mathbf{X}', \mathbf{V} - \mathbf{V}') d\mathbf{X}' d\mathbf{V}' d\mathbf{X} d\mathbf{V}, \end{aligned}$$

where in the first identity we denoted $\mathbf{X}'' = \mathbf{X} + \mathbf{X}'$, $\mathbf{V}'' = \mathbf{V} + \mathbf{V}'$, and in the second we re-denoted \mathbf{X} as \mathbf{X}' , \mathbf{V} as \mathbf{V}' , \mathbf{X}'' as \mathbf{X} , and \mathbf{V}'' as \mathbf{V} . Second, we note that

$$(2.9) \quad \begin{aligned} \int g(\mathbf{X}, \mathbf{V}) F(\mathbf{X}, \mathbf{V}) \pi(\mathbf{X}, \mathbf{V}, \mathbf{X}', \mathbf{V}') d\mathbf{X}' d\mathbf{V}' d\mathbf{X} d\mathbf{V} &= \\ &= \int g(\mathbf{X}, \mathbf{V}) F(\mathbf{X}, \mathbf{V}) \pi(\mathbf{X}, \mathbf{V}, \mathbf{X}' - \mathbf{X}, \mathbf{V}' - \mathbf{V}) d\mathbf{X}' d\mathbf{V}' d\mathbf{X} d\mathbf{V}. \end{aligned}$$

Finally, we denote

$$(2.10) \quad \pi(\mathbf{X}, \mathbf{V}, \mathbf{X}', \mathbf{V}') \equiv F_{cond}(\mathbf{X} + \mathbf{X}', \mathbf{V} + \mathbf{V}' | \mathbf{X}, \mathbf{V}),$$

where $F_{cond}(\mathbf{X}_a, \mathbf{V}_a | \mathbf{X}_b, \mathbf{V}_b)$ is the conditional probability that \mathbf{X} and \mathbf{V} equal \mathbf{X}_a and \mathbf{V}_a after the jump, respectively, given that their states were, respectively, \mathbf{X}_b and \mathbf{V}_b before the jump. Substituting the results into (2.6) and peeling off the integrals against $g d\mathbf{X} d\mathbf{V}$, we recover the forward Kolmogorov equation in the form

$$(2.11) \quad \frac{\partial F}{\partial t} + \mathbf{V} \cdot \nabla_{\mathbf{X}} F = \int [F_{cond}(\mathbf{X}, \mathbf{V} | \mathbf{X}', \mathbf{V}') F(\mathbf{X}', \mathbf{V}') - F_{cond}(\mathbf{X}', \mathbf{V}' | \mathbf{X}, \mathbf{V}) F(\mathbf{X}, \mathbf{V})] d\mathbf{X}' d\mathbf{V}'.$$

The integral in the right-hand side is the main part of the master equation [23].

At this point, we observe that the coordinates \mathbf{X} of all particles do not change during the collisions. This sets the form of $F_{cond}(\mathbf{X}, \mathbf{V}|\mathbf{X}', \mathbf{V}')$ to

$$(2.12) \quad F_{cond}(\mathbf{X}, \mathbf{V}|\mathbf{X}', \mathbf{V}') = F_{cond}(\mathbf{V}|\mathbf{V}')\delta(\mathbf{X} - \mathbf{X}'),$$

where $F_{cond}(\mathbf{V}|\mathbf{V}')$, of course, depends on \mathbf{X} , but we do not express it explicitly for the sake of brevity. Subsequently, the collision integral can be contracted in \mathbf{X}' as

$$(2.13) \quad \int [F_{cond}(\mathbf{X}, \mathbf{V}|\mathbf{X}', \mathbf{V}')F(\mathbf{X}', \mathbf{V}') - F_{cond}(\mathbf{X}', \mathbf{V}'|\mathbf{X}, \mathbf{V})F(\mathbf{X}, \mathbf{V})] d\mathbf{X}' d\mathbf{V}' = \\ = \int [F_{cond}(\mathbf{V}|\mathbf{V}')F(\mathbf{V}') - F_{cond}(\mathbf{V}'|\mathbf{V})F(\mathbf{V})] d\mathbf{V}',$$

where we write $F(\mathbf{V}) \equiv F(\mathbf{X}, \mathbf{V})$ and $F(\mathbf{V}') \equiv F(\mathbf{X}, \mathbf{V}')$, again, for the sake of brevity.

Now, we need to impose the appropriate reversibility conditions on F_{cond} , which must hold from the considerations of physics. First, we assume that if all particle velocities in the system are instantaneously reversed, the system must generally retrace its steps backwards, which implies $F_{cond}(\mathbf{V}|\mathbf{V}') = F_{cond}(-\mathbf{V}'|-\mathbf{V})$. Second, we also assume that F_{cond} must remain invariant if we flip the sign of the time variable; this implies $F_{cond}(\mathbf{V}|\mathbf{V}') = F_{cond}(-\mathbf{V}|-\mathbf{V}')$. Together, these two relations yield the following reversibility condition:

$$(2.14) \quad F_{cond}(\mathbf{V}|\mathbf{V}') = F_{cond}(\mathbf{V}'|\mathbf{V}).$$

With this, the forward Kolmogorov equation takes the form

$$(2.15) \quad \frac{\partial F}{\partial t} + \mathbf{V} \cdot \nabla_{\mathbf{X}} F = \int F_{cond}(\mathbf{V}|\mathbf{V}') [F(\mathbf{V}') - F(\mathbf{V})] d\mathbf{V}'.$$

We can immediately see that a uniform distribution on the constant momentum-energy sphere turns the collision term in the right-hand side of the Kolmogorov equation (2.15) into zero; in what follows, we will assume that this is also the only such distribution, that is, the motion on the constant momentum-energy sphere is ergodic.

The next step is to assume that only two particles collide during any given collision event. Without much loss of generality, we assume that the first and second particles collide, while the rest do not interact and their velocities do not change. This leads to

$$(2.16) \quad F_{cond}(\mathbf{V}|\mathbf{V}') = f_{cond}(\mathbf{v}, \mathbf{v}_2|\mathbf{v}', \mathbf{v}_2')\delta(\mathbf{x}_2 - \mathbf{x})\delta(\mathbf{v}_3' - \mathbf{v}_3) \dots \delta(\mathbf{v}_K' - \mathbf{v}_K),$$

where $\delta(\mathbf{x}_2 - \mathbf{x})$ is necessary since the coordinates of the first and second particles have to be identical during the collision. Of course, in reality gas particles have finite sizes, and thus their coordinates do not have to coincide precisely for them to interact, which means that this delta-function above is in effect a very tall and narrow, but finite, distribution. However, formally the delta-function suffices for the purpose, since the integration over \mathbf{x}_2 will be carried out below. This further yields

$$(2.17) \quad \int F_{cond}(\mathbf{V}|\mathbf{V}') [F(\mathbf{V}') - F(\mathbf{V})] d\mathbf{V}' = \delta(\mathbf{x}_2 - \mathbf{x}) \cdot \\ \cdot \int f_{cond}(\mathbf{v}, \mathbf{v}_2|\mathbf{v}', \mathbf{v}_2') [F(\mathbf{v}', \mathbf{v}_2', \mathbf{v}_3, \dots, \mathbf{v}_K) - F(\mathbf{v}, \mathbf{v}_2, \mathbf{v}_3, \dots, \mathbf{v}_K)] d\mathbf{v}' d\mathbf{v}_2'.$$

Now, we denote the second marginal of F as

$$(2.18) \quad f^{(2)} = \int F \, dx_3 \dots dx_K \, dv_3 \dots dv_K.$$

Then, integrating the forward Kolmogorov equation over all particles except for the first two yields

$$(2.19) \quad \frac{\partial f^{(2)}}{\partial t} + (v, v_2) \cdot \nabla_{(x, x_2)} f^{(2)} = \delta(x_2 - x) \int f_{cond}(v, v_2 | v', v'_2) \left[f^{(2)}(x, v', x_2, v'_2) - f^{(2)}(x, v, x_2, v_2) \right] dv' dv'_2.$$

Above, we, of course, used the fact that the integrals over $x_3 \dots x_K$ against corresponding x -derivatives canceled themselves out. The next step is to integrate over the second particle to get the first marginal (that is, the single-particle distribution). We denote

$$(2.20) \quad f = \int f^{(2)} \, dx_2 \, dv_2.$$

Then, further integrating the Kolmogorov equation above over x_2 and v_2 yields

$$(2.21) \quad \frac{\partial f}{\partial t} + v \cdot \nabla_x f = \int f_{cond}(v, v_2 | v', v'_2) \left[f^{(2)}(x, v', x, v'_2) - f^{(2)}(x, v, x, v_2) \right] dv' dv'_2 dv_2,$$

which, after the factorization of $f^{(2)}$ into the product of two single-particle distributions, results in

$$(2.22) \quad \frac{\partial f}{\partial t} + v \cdot \nabla_x f = \int f_{cond}(v, v_2 | v', v'_2) \left[f(v') f(v'_2) - f(v) f(v_2) \right] dv' dv'_2 dv_2.$$

Next, we recall that jumps preserve the total energy and total momentum of the system of all particles. For the two colliding particles (with velocities v and v_2 before the jump, and v' and v'_2 after the jump) this means that

$$(2.23) \quad v + v_2 = v' + v'_2, \quad \|v\|^2 + \|v_2\|^2 = \|v'\|^2 + \|v'_2\|^2,$$

that is, if v and v_2 are prescribed, then the possible states of v' and v'_2 are restricted by these conservation laws. These conservation laws can be rearranged in the form

$$(2.24) \quad v' = v - (\omega \cdot (v - v_2))\omega, \quad v'_2 = v_2 + (\omega \cdot (v - v_2))\omega,$$

where ω is an arbitrary unit vector. With the new restrictions, the integrals over $dv' dv'_2$ are replaced with the ω -integral over a unit sphere:

$$(2.25) \quad \frac{\partial f}{\partial t} + v \cdot \nabla_x f = \int f_{cond}(v', v'_2 | v, v_2) \left[f(v') f(v'_2) - f(v) f(v_2) \right] d\omega dv_2.$$

Observe that the result is the usual Boltzmann equation in (1.1) with the collision term in (1.2), where the collision kernel B is specified by f_{cond} .

Remark. There seems to be a contradiction between the requirement that the system of particles in (2.2) as a whole preserves the momentum and energy, and the above factorization of $f^{(2)}$ into the product of its marginals f . The reason is that the factorization

implies that the particles are independently distributed, while the momentum and energy conservation laws effectively preclude it. Here we clarify that the above derivation was done under the assumption that the total number of particles K was so large, that even given the fact that all particles together were bound by the momentum and energy conservation laws, any given pair of them was effectively statistically independent.

3. LONG-TERM BEHAVIOR OF THE RANDOM PARTICLE SYSTEM

Here we look at the long-term behavior of the random jump system in (2.2) using the standard multiscale expansion methods [3, 24, 31, 37]. From what we know about gases, there exist two scales of evolution of the dynamical system in (2.2). The “microscale” of evolution occurs locally (on the space scale of a few mean paths), where particles reach their local statistical equilibrium almost immediately, with particle velocities distributed according to the Maxwell-Boltzmann distribution, and their locations distributed evenly. At the same time, on the “macroscale” of evolution the parameters of the microscale distribution F can vary throughout the space, and typically evolve on a much slower time scale. With this observation, we should formally consider $V(t)$ a fast process: $V(t) \rightarrow V(t/\varepsilon)$, where $0 < \varepsilon \ll 1$ is a small scaling parameter.

However, such a direct rescaling would cause a technical inconvenience: observe that, in the limit as $\varepsilon \rightarrow 0$, X becomes a constant parameter in the jump process $N(t)$, which governs the velocity. In the previous section we found that the jump measure Π depends on the coordinates of the particles, and in particular, it requires that the coordinates of two particles coincide for a jump to occur. So, if X is fixed, then either no jumps occur at all, or two same particles repeatedly jump every time the jump arrives. In order to circumvent this issue, we use an approach somewhat similar to the one in the book by Pavliotis and Stuart [31], Section 11.7.5. First, we rename X as Y , so that Y now plays the role of the microscale coordinate, and the jumps in $N(t)$ depend on it. Second, we introduce the macroscale coordinate $X \sim \varepsilon Y$. Third, we rescale time as $t \rightarrow \varepsilon t$. This trick allows us to “accelerate” $V(t) \rightarrow V(t/\varepsilon)$ without losing jumps. With the rescaling above, the dynamical system in (2.2) can be written as

$$(3.1) \quad \frac{dX}{dt} = V,$$

where the process V is produced by

$$(3.2) \quad \frac{dY}{dt} = \frac{1}{\varepsilon} V, \quad dV = dN(t/\varepsilon), \quad \text{with jumps in } N(t) \text{ dependent on } Y.$$

Strictly speaking, such a space-time scale separation is not necessarily inherently present in any gas dynamics. For example, in the upper portions of the Earth atmosphere the air is so rarefied, that the time and distance between collisions becomes comparable to the macroscale times and distances. Therefore, what follows below applies only in situations which are sufficiently close to “normal conditions”, or at least far from the extent of the rarefaction where the two scales of evolution merge into one.

Substituting the ansatz in (3.1) and (3.2) into the Kolmogorov equation in (2.15), we obtain

$$(3.3a) \quad \frac{\partial F}{\partial t} + \mathbf{V} \cdot \nabla_{\mathbf{X}} F = \frac{1}{\varepsilon} \mathcal{L}_0^* F,$$

$$(3.3b) \quad \mathcal{L}_0^* F = \int F_{cond}(\mathbf{V}|\mathbf{V}') [F(\mathbf{V}') - F(\mathbf{V})] d\mathbf{V}' - \mathbf{V} \cdot \nabla_{\mathbf{Y}} F.$$

Observe that, in the zero- ε limit, F becomes an equilibrium state for \mathcal{L}_0^* . One can find, by inspection, that any F , constant in \mathbf{Y} and on the \mathbf{V} -sphere of constant momentum and energy, is automatically an equilibrium state for \mathcal{L}_0^* . In what follows, we will assume that it is also the *only* such state, that is, the process (\mathbf{Y}, \mathbf{V}) is ergodic. By ν , we will denote the uniform invariant measure of (\mathbf{Y}, \mathbf{V}) . The projection of such a measure onto the velocity of a single particle approaches the Gaussian density in the many-particle limit, which further suggests the “compatibility” of the jump process with the Boltzmann equation, since the canonical Maxwell-Boltzmann equilibrium state is also given by the Gaussian distribution.

Below, a bar over a probability density will denote the (\mathbf{Y}, \mathbf{V}) -average

$$(3.4) \quad \bar{F} = \int F d\mathbf{Y} d\mathbf{V}.$$

In what follows, the exact form of \mathcal{L}_0^* is unimportant, as long as it has the necessary properties above. Our goal at this point is to compute the leading order Kolmogorov operator for F , which is independent of ε . We expand F as

$$(3.5) \quad F = F_0 + \varepsilon F_1 + \dots,$$

which produces the forward Kolmogorov equation in the form

$$(3.6) \quad \left(\frac{\partial}{\partial t} + \mathbf{V} \cdot \nabla_{\mathbf{X}} - \frac{1}{\varepsilon} \mathcal{L}_0^* \right) (F_0 + \varepsilon F_1 + \dots) = 0.$$

The identity above should hold for any value of ε , and thus results in a set of equations, one for each power of ε separately. We now examine these equations starting with the lowest order in ε .

- **Order ε^{-1} .** For this order, we simply recover

$$(3.7) \quad \mathcal{L}_0^* F_0 = 0.$$

We conclude that F_0 belongs to the null space of \mathcal{L}_0^* , that is, F_0/\bar{F}_0 is the density of ν :

$$(3.8) \quad \int g F_0 d\mathbf{Y} d\mathbf{V} = \bar{F}_0 \int g d\nu, \quad \text{for any suitable function } g.$$

- **Order ε^0 .** Here we have

$$(3.9) \quad \frac{\partial F_0}{\partial t} = -\mathbf{V} \cdot \nabla_{\mathbf{X}} F_0 + \mathcal{L}_0^* F_1.$$

Then, integrating over $d\mathbf{Y} d\mathbf{V}$, for \bar{F}_0 we obtain

$$(3.10) \quad \frac{\partial \bar{F}_0}{\partial t} = - \int \mathbf{V} \cdot \nabla_{\mathbf{X}} F_0 d\mathbf{Y} d\mathbf{V} + \int \mathcal{L}_0^* F_1 d\mathbf{Y} d\mathbf{V}.$$

The second term in the right-hand side above can be expressed as

$$(3.11) \quad \int \mathcal{L}_0^* F_1 dY dV = \int 1 \mathcal{L}_0^* F_1 dY dV = \int F_1 \mathcal{L}_0 1 dY dV = 0,$$

since 1 belongs to the (one-dimensional, due to the ergodicity assumption) null space of the corresponding generator \mathcal{L}_0 . We therefore have

$$(3.12) \quad \frac{\partial \bar{F}_0}{\partial t} = -\operatorname{div}_X \int V F_0 dY dV = -\operatorname{div}_X \left(\bar{F}_0 \int V d\nu \right) = -\operatorname{div}_X (\bar{F}_0 \mathbf{U}_0),$$

where we defined the limiting average velocity \mathbf{U}_0 as

$$(3.13) \quad \mathbf{U}_0 = \int V d\nu.$$

Thus, the effective long-term averaged dynamics for \mathbf{X} are provided by

$$(3.14) \quad \frac{d\bar{\mathbf{X}}}{dt} = \mathbf{U}_0.$$

3.1. Centered process. Using the averaged quantities $\bar{\mathbf{X}}$ and \mathbf{U}_0 , computed above, here we introduce the centered coordinate \mathbf{X}^c and velocity \mathbf{V}^c as

$$(3.15) \quad \mathbf{X}^c = \mathbf{X} - \bar{\mathbf{X}}, \quad \mathbf{V}^c = \mathbf{V} - \mathbf{U}_0,$$

respectively. We also introduce the new, centered probability distribution F^c via the identity

$$(3.16) \quad F^c(t, \mathbf{X}^c, \mathbf{V}^c) \equiv F(t, \mathbf{X}, \mathbf{V}).$$

Then, one can see that

$$(3.17) \quad \frac{\partial F}{\partial t} = \frac{\partial F^c}{\partial t} - \mathbf{U}_0 \cdot \nabla_{\mathbf{X}} F^c, \quad \mathbf{V} \cdot \nabla_{\mathbf{X}} F = (\mathbf{V}^c + \mathbf{U}_0) \cdot \nabla_{\mathbf{X}} F^c,$$

which leads to the centered Kolmogorov equation in the form

$$(3.18) \quad \frac{\partial F^c}{\partial t} + \mathbf{V}^c \cdot \nabla_{\mathbf{X}} F^c = \frac{1}{\varepsilon} \mathcal{L}_0^* F^c.$$

Clearly, the long-term dynamics of \mathbf{X}^c manifest at the higher order of ε , since it is already centered at its averaging limit. For that, we expand the corresponding centered probability density F^c in the higher-order as

$$(3.19) \quad F^c = F_0^c + \varepsilon F_1^c + \varepsilon^2 F_2^c + \dots,$$

which, upon substitution into (3.18), yields

$$(3.20) \quad \left(\frac{\partial}{\partial t} + \mathbf{V}^c \cdot \nabla_{\mathbf{X}} - \frac{1}{\varepsilon} \mathcal{L}_0^* \right) (F_0^c + \varepsilon F_1^c + \varepsilon^2 F_2^c + \dots) = 0.$$

We again look at the identities for different orders of ε .

- **Order ε^{-1} .** Here we similarly obtain

$$(3.21) \quad \mathcal{L}_0^* F_0^c = 0,$$

that is, F_0^c / \bar{F}_0^c is the density of the centered invariant probability measure ν^c . Here, ν^c is the uniform invariant probability measure on the union of the Y -space, and the zero-momentum, constant energy sphere in the V^c -space.

- **Order ε^0 .** The time-derivative of \bar{F}^c is of higher order in ε , so for the current order we obtain the equation

$$(3.22) \quad \mathcal{L}_0^* F_1^c = V^c \cdot \nabla_X F_0^c,$$

whose solutions are defined up to an additive term cF_0^c with an arbitrary constant c , since F_0^c is in the null space of \mathcal{L}_0^* . Below we will show how to choose a specific F_1^c that we need, out of many possible solutions.

- **Order ε .** Here we obtain

$$(3.23) \quad \frac{1}{\varepsilon} \frac{\partial F_0^c}{\partial t} = -V^c \cdot \nabla_X F_1^c + \mathcal{L}_0^* F_2^c.$$

For \bar{F}_0^c we integrate over $dY dV^c$ as

$$(3.24) \quad \frac{1}{\varepsilon} \frac{\partial \bar{F}_0^c}{\partial t} = -\operatorname{div}_X \int F_1^c V^c dY dV^c + \int \mathcal{L}_0^* F_2^c dY dV^c,$$

where, as before, the last integral is zero, for the same reasons.

As before, we need to determine the closed equation for \bar{F}_0^c . For that, we denote by Φ a solution to the problem

$$(3.25) \quad \mathcal{L}_0 \Phi = V^c,$$

which is defined up to an additive constant due to the null-space of \mathcal{L}_0 . Then, we can formally write

$$(3.26) \quad \int F_1^c V^c dY dV^c = \int F_1^c \mathcal{L}_0 \Phi dY dV^c = \int \Phi \mathcal{L}_0^* F_1^c dY dV^c = \int \Phi (V^c \cdot \nabla_X F_0^c) dY dV^c.$$

To solve for Φ , let us define the process $Z(t, V^c)$ as

$$(3.27) \quad Z(t, V^c) = \int_0^t \mathbb{E} V^c(s) ds, \quad V^c(0) = V^c,$$

where the symbol \mathbb{E} denotes the expectation over the probability space of the random jump process $N(t)$, with uniformly distributed initial conditions for Y . Then, by the definition of the generator \mathcal{L}_0 ,

$$(3.28) \quad \begin{aligned} \mathcal{L}_0 Z(t, V^c) &= \lim_{h \rightarrow 0} \frac{\mathbb{E} Z(t, V^c(h)) - Z(t, V^c)}{h} = \\ &= \lim_{h \rightarrow 0} \frac{1}{h} \left(\int_h^{t+h} \mathbb{E} V^c(s) ds - \int_0^t \mathbb{E} V^c(s) ds \right) = \\ &= \lim_{h \rightarrow 0} \frac{1}{h} \left(\int_t^{t+h} \mathbb{E} V^c(s) ds - \int_0^h \mathbb{E} V^c(s) ds \right) = \mathbb{E} V^c(t) - V^c. \end{aligned}$$

Observing that $\mathbb{E}V^c(t) \rightarrow \mathbf{0}$ in the limit as $t \rightarrow \infty$ (since, by ergodicity, the expectation becomes the average over v^c in the infinite time limit), we obviously arrive at the solution Φ in the form

$$(3.29) \quad \Phi = -\lim_{t \rightarrow \infty} \mathbf{Z}(t, V^c) + \mathbf{C} = -\int_0^\infty \mathbb{E}V^c(s) ds + \mathbf{C},$$

where \mathbf{C} is a vector which does not depend on V^c . The term F_1^c should, therefore, be chosen to satisfy the normalization

$$(3.30) \quad \int F_1^c V^c dY dV^c = -\int_0^\infty ds \int \mathbb{E}V^c(s) (V^c \cdot \nabla_X F_0^c) dY dV^c,$$

since

$$(3.31) \quad \int \mathbf{C} (V^c \cdot \nabla_X F_0^c) dY dV^c = \mathbf{C} \operatorname{div}_X \int F_0^c V^c dY dV^c = \mathbf{C} \operatorname{div}_X \left(\bar{F}_0^c \int V^c dv^c \right) = \mathbf{0}.$$

The choice of \mathbf{C} is, therefore, irrelevant. As a result, the equation for \bar{F}_0^c reads

$$(3.32) \quad \begin{aligned} \frac{\partial \bar{F}_0^c}{\partial t} &= \varepsilon \operatorname{div}_X \int_0^\infty ds \int \mathbb{E}V^c(s) (V^c \cdot \nabla_X F_0^c) dY dV^c = \\ &= \operatorname{div}_X \int_0^\infty ds \int \mathbb{E}V^c(s/\varepsilon) (V^c \cdot \nabla_X F_0^c) dY dV^c, \end{aligned}$$

where we moved the small scaling parameter ε into the argument of V^c in the right-hand side, since it was stated in (3.1) and (3.2) that formally the velocity was a fast process. Now we need to look for a practically tractable form of the right-hand side of the long-term Kolmogorov equation. For that, we introduce two simplifications of the velocity correlation function above, which are suitable for processes with many statistically independent and identically distributed particles. First, we assume that

$$(3.33) \quad \int V^c \otimes V^c dv^c = \theta_0 \mathbf{I},$$

where “ \otimes ” stands for the outer product of two vectors. Above, θ_0 is the temperature of the thermodynamic equilibrium state F_0 (expressed in the velocity-squared units), and \mathbf{I} is an identity matrix. The explicit formula for θ_0 is then given by

$$(3.34) \quad \theta_0 = \frac{1}{KN} \int \|V^c\|^2 dv^c = \frac{1}{KN} \int \|V - U_0\|^2 dV.$$

Second, we assume that the integral over the time series of $\mathbb{E}V^c(t/\varepsilon)$ is proportional to the initial state V^c :

$$(3.35) \quad \int_0^\infty \mathbb{E}V^c(s/\varepsilon) ds = \tau_0 V^c,$$

where τ_0 is the characteristic decay time which does not depend on V^c . The common sense behind this assumption is that, since, for $\varepsilon \rightarrow 0$ in the centered Kolmogorov equation (3.18), V^c is a compound Poisson process on the sphere of zero momentum and constant energy with otherwise equiprobable jumps in all directions, its expectation should directly approach the center of the sphere as time increases, at the rate which

does not depend on a particular initial condition. Since the process V^c is centered, the expectation of the process must be a multiple of its initial displacement from zero.

We expect $\tau_0 \ll 1$, since it includes a time integral over the expectation of the fast, rapidly decorrelating centered velocity process. Under the assumptions above, the explicit formula for τ_0 is given by the time integral over the autocorrelation function

$$(3.36) \quad \tau_0 = \frac{1}{KN\theta} \int_0^\infty ds \int \mathbb{E} V^c(s/\varepsilon) \cdot V^c d\nu^c = \\ = \frac{1}{KN\theta} \int_0^\infty ds \int (\mathbb{E} V(s/\varepsilon) - \mathbf{u}_0) \cdot (V - \mathbf{u}_0) d\nu.$$

These two assumptions yield

$$(3.37) \quad \int_0^\infty ds \int \mathbb{E} V^c(s/\varepsilon) (V^c \cdot \nabla_X F_0^c) dY dV^c = \tau_0 \int V^c \otimes V^c \nabla_X F_0^c dY dV^c = \\ = \tau_0 \operatorname{div}_X \left(\bar{F}_0^c \int V^c \otimes V^c d\nu^c \right) = \tau_0 \nabla_X (\theta_0 \bar{F}_0^c).$$

This, in turn, leads to the final form of the long-term Kolmogorov equation for the centered coordinate process X^c :

$$(3.38) \quad \frac{\partial \bar{F}_0^c}{\partial t} = \operatorname{div}_X (\tau_0 \nabla_X (\theta_0 \bar{F}_0^c)).$$

The equation above can also be rewritten as

$$(3.39) \quad \frac{\partial \bar{F}_0^c}{\partial t} + \operatorname{div}_X (\theta_0 \bar{F}_0^c \nabla_X \tau_0) = \Delta_X (\tau_0 \theta_0 \bar{F}_0^c),$$

where $\Delta_X = \nabla_X \cdot \nabla_X$ is the usual Laplace operator. The effective long-term homogenization dynamics for the corresponding centered process X^c is, therefore, given by the Itô stochastic differential equation [30]

$$(3.40) \quad d\bar{X}^c = \theta_0 \nabla_X \tau_0 dt + \sqrt{2\tau_0 \theta_0} dW(t),$$

where $W(t)$ is a KN -dimensional Wiener process.

4. THE DIFFUSIVE BOLTZMANN EQUATION

The conventional Boltzmann equation in (1.1) is derived under the number of idealizing assumptions on the collisions of the particles, which in reality do not hold for the real gas molecules. Some of the examples are the following:

- In the Boltzmann equation, it is assumed that the particles are independently and identically distributed even after they collide. However, the real gas molecules, even if distributed statistically independently prior to any collisions, must become statistically correlated to some extent after they collide, since they have exchanged their information through interaction.
- In the Boltzmann equation, it is assumed that at most two particles can collide at once. However, in reality there could be events when three (or more) real gas molecules collide at once.

- Near a wall, real gas molecules also collide with the molecules of the wall, which is a solid physical object, where molecules behave in a completely different manner. This “influence of the wall” extends somewhat away from the wall via subsequent collisions of the deflected molecules with those which did not interact with the wall. The collision operator in the Boltzmann equation has no provision for such collisions.

A straightforward way to take into account these effects is to develop a more comprehensive collision model with additional complexity. However, while it could potentially be possible to do this, it might not necessarily be practical. For example, accounting for post-collision statistical dependence of two particles is not necessarily possible in a single-particle distribution framework of the Boltzmann equation, and likely requires a sort of a multi-particle model, perhaps a (heavily simplified) version of (2.2). Also, incorporating the actual molecular walls (or some simplified analogs) into the model would likely make the model too complicated for the majority of practical applications, where one usually aims to treat the walls as the abstract “boundaries” of the domain where the properties of the gas can be specified however needed.

Here we propose another, in a certain sense opposite, approach, which is to introduce an “imperfection” into the existing collision model (in the form of a lack of certain information on collisions) without changing its basic conceptual framework, and to compensate this imperfection in an approximate way. However, such an imperfection must be described in statements which are already “known” to the model, to avoid creating a new model. Here, the collision model is very simple, essentially consisting of fundamental conservation laws (which we obviously cannot discard) and otherwise random collision outcomes, thus there is not much we can assume to be lacking. Effectively, the only aspect of model collisions that we can subvert is the very occurrence (or capture, in the model context) of collisions, since *that* is not conventionally elaborated upon, as it is implied that particles somehow collide whenever they collide. So, we are going to assume that not all collisions are accounted for by the model collision term, and that, accordingly, the velocity jump process randomly misses some collisions, albeit in a sufficiently unbiased fashion.

Assumption 1. *A model of particle collisions, expressed through the random jump process in (2.2), does not track all collisions, but rather some of them. However, the collisions are missed in a sufficiently unbiased way, so that the averaging limits (3.14) of the real process and the model are identical. As a result, the effect of missed collisions manifests on the longer time scale of the homogenization process in (3.40).*

In order to account for the missed jumps, we propose to use the scaled (empirically, for now) centered homogenization process from (3.40) as a statistical correction to the particle coordinate X in the original random jump process in (2.2) as follows:

$$(4.1) \quad dX = (V + \theta_\alpha \nabla_X \tau_\alpha) dt + \sqrt{2\tau_\alpha \theta_\alpha} dW(t), \quad dV = dN(t),$$

where θ_α and τ_α denote the appropriately scaled versions of θ_0 and τ_0 . Here, we assume that the scaling parameter $\alpha > 0$ only adjusts the bulk statistical spread (also called the standard deviation) of the velocity distribution v , leaving all other properties the same.

This constant scaling may be an oversimplification in some practical situations, since the effect of “imperfection” should, for example, likely be stronger closer to the walls rather than away from them. Nevertheless, below we show that even this simple scaling assumption yields rather interesting results. A variable scaling, possibly emerging from an appropriate kinetic analog of the turbulent energy [28, 29] assuming the role of θ_α , will be addressed in the future work.

The corresponding forward Kolmogorov equation from (2.15) for the new system in (4.1) becomes

$$(4.2) \quad \frac{\partial F}{\partial t} + \mathbf{V} \cdot \nabla_{\mathbf{X}} F = \int F_{\text{cond}}(\mathbf{V}|\mathbf{V}') [F(\mathbf{V}') - F(\mathbf{V})] d\mathbf{V}' + \text{div}_{\mathbf{X}} (\tau_\alpha \nabla_{\mathbf{X}} (\theta_\alpha F)).$$

Following the same steps as in Section 2, from the Kolmogorov equation in (4.2) we obtain the diffusive Boltzmann equation

$$(4.3) \quad \frac{\partial f}{\partial t} + \mathbf{v} \cdot \nabla_{\mathbf{x}} f = \mathcal{C}(f) + \text{div}_{\mathbf{x}} (\tau_\alpha \nabla_{\mathbf{x}} (\theta_\alpha f)).$$

Below we will show computationally that the corresponding fluid dynamics equations, emerging from the diffusive Boltzmann equation above in (4.3), exhibit some interesting properties not found in the conventional fluid dynamics equations.

4.1. Approximations for the scaled temperature and decay time. Here we assume that θ_α and τ_α result from θ_0 and τ_0 by empirically scaling the statistical spread of the particle velocities (the standard deviation from the mean velocity) by α . As a result, the homogenization dynamics provided by θ_α and τ_α are qualitatively the same as those in (3.40).

Observe that the formulas for θ_0 and τ_0 in (3.34) and (3.36), respectively, are given by the multi-particle integrals over the limiting measure ν . However, the diffusive Boltzmann equation in (4.3) no longer has access to the multi-particle limiting dynamics. Thus, suitable approximations for θ_0 and τ_0 via the one-particle distribution f of the diffusive Boltzmann equation are needed. For that, we first need to introduce a concise notation of an arbitrary statistical moment of the single-particle distribution function f from the diffusive Boltzmann equation in (4.3). Let $g(\mathbf{v})$ be an integrable (with respect to f) function of \mathbf{v} . We then denote

$$(4.4) \quad \langle g \rangle_f(t, \mathbf{x}) = \int g f d\mathbf{v}, \quad \langle g \rangle_{\mathcal{C}(f)}(t, \mathbf{x}) = \int g \mathcal{C}(f) d\mathbf{v},$$

where $\mathcal{C}(f)$ is the Boltzmann collision operator. Now, we write the density ρ , flow velocity \mathbf{u} and temperature θ as

$$(4.5) \quad \rho = \langle 1 \rangle_f, \quad \mathbf{u} = \frac{1}{\rho} \langle \mathbf{v} \rangle_f, \quad \theta = \frac{1}{N\rho} \langle \|\mathbf{v} - \mathbf{u}\|^2 \rangle_f = \frac{1}{N} \left(\frac{1}{\rho} \langle \|\mathbf{v}\|^2 \rangle_f - \|\mathbf{u}\|^2 \right),$$

where $\langle \mathbf{v} \rangle_f$ is the momentum, and one-half of $\langle \|\mathbf{v}\|^2 \rangle_f$ is the energy. Our first approximation here is quite straightforward:

$$(4.6) \quad \theta_0 \approx \theta.$$

Indeed, observe that if all particles in (3.34) and (3.36) are statistically independent and identically distributed, their individual moments are also identical. The “ \approx ” sign is, however, due to the fact that f is not a projection of a limiting measure ν onto a single

particle, but rather the projection of the full (X, V) -dependent measure F . However, if the dynamics for X and V are indeed strongly time-scale separated, then the velocity moments of F (and, therefore, f) can be approximately treated as if they were the moments of ν . The scaled temperature θ_α is, therefore, given by

$$(4.7) \quad \theta_\alpha \approx \alpha^2 \theta,$$

since the statistical spread (standard deviation) is proportional to the square root of the temperature.

As far as the characteristic decay time τ_0 is concerned, one should generally be able to evaluate it from the properties of the Lévy measure Π of the jump process $N(t)$, and the diameter of the constant momentum-energy sphere on which this jump process lives. However, for the simplicity of the presentation, here we will use a crude, heuristic approximation for τ_0 . Observe that τ_0 is proportional to the average time which passes between the jumps in the process $N(t)$. For example, if we set the jumps to happen twice as often (being same otherwise), then the characteristic decay time, being the time integral over the velocity jump process, will accordingly become twice as short. Thus, we are going to use the approximations of the kinetic theory [13] for the characteristic decay time. Observe that

$$(4.8) \quad \tau_0 \sim \langle \text{mean time between jumps} \rangle \sim \frac{\langle \text{mean free path} \rangle}{\langle \text{mean speed} \rangle}.$$

On the other hand

$$(4.9) \quad \langle \text{mean free path} \rangle \sim \frac{1}{\rho}, \quad \langle \text{mean speed} \rangle \sim \sqrt{\theta}.$$

Thus, we conclude that the characteristic time τ_0 and its scaled version τ_α are given, respectively, by

$$(4.10) \quad \tau_0 \sim \frac{1}{\rho\sqrt{\theta}}, \quad \tau_\alpha \sim \frac{1}{\alpha\rho\sqrt{\theta}}.$$

Thus, under the assumption that α is constant, the additional diffusion term in the diffusive Boltzmann equation (4.3) scales as

$$(4.11) \quad \text{div}_x (\tau_\alpha \nabla_x (\theta_\alpha f)) \sim \text{div}_x \left(\frac{\alpha}{\rho\sqrt{\theta}} \nabla_x (\theta f) \right).$$

Introducing the dynamic mass diffusivity D and its empirical scaled version D_α as

$$(4.12) \quad D = \tau_0 \rho \theta, \quad D_\alpha = \alpha D,$$

we write the diffusive Boltzmann equation in (4.3) as

$$(4.13) \quad \frac{\partial f}{\partial t} + v \cdot \nabla_x f = \mathcal{C}(f) + \text{div}_x \left(\frac{D_\alpha}{\rho\theta} \nabla_x (\theta f) \right).$$

The scaled dynamic mass diffusivity D_α can be specified empirically as

$$(4.14) \quad D_\alpha = D_\alpha^* \sqrt{\frac{\theta}{\theta^*}},$$

where D_α^* is a given (heuristically chosen, fitted, or, perhaps, somehow measured) scaled diffusivity for a reference state θ^* .

5. THE DIFFUSIVE FLUID DYNAMICS EQUATIONS

Here we integrate the diffusive Boltzmann equation against different powers of the velocity \mathbf{v} , obtaining the equations for different velocity moments of the distribution density f . This is a standard procedure, which, for the usual Boltzmann equation in (1.1), leads to the conventional equations of gas dynamics, such as the Euler and Grad equations [4, 20, 21, 26].

Integrating the diffusive Boltzmann equation in (4.13) against a moment $g(\mathbf{v})$ in \mathbf{v} , and using the notations from the previous section, we obtain

$$(5.1) \quad \frac{\partial \langle g \rangle_f}{\partial t} + \operatorname{div} \langle g \mathbf{v} \rangle_f = \langle g \rangle_{\mathcal{C}(f)} + \operatorname{div} \left(\frac{D_\alpha}{\rho \theta} \nabla (\theta \langle g \rangle_f) \right),$$

where we drop the subscript “ \mathbf{x} ” from the differentiation operators, since the \mathbf{v} -variable is no longer in the equation. It is interesting that the additional term in the right-hand side can be separated into the diffusion and transport terms as

$$(5.2) \quad \operatorname{div} \left(\frac{D_\alpha}{\rho \theta} \nabla (\theta \langle g \rangle_f) \right) = \operatorname{div} \left(\frac{D_\alpha}{\rho} (\nabla \langle g \rangle_f + \langle g \rangle_f \nabla \ln \theta) \right),$$

which, together, constitute a simple linearized thermophoretic transport-diffusion process with the Soret coefficient [16] set to θ^{-1} . In the earlier works on the extended fluid dynamics [6–8, 14], the transport terms due to the temperature gradient are not present. Surprisingly, in [15, 17] the temperature gradient transport terms are present, however, they appear to be of a form different from the one above.

Observe that the moment equation above in (5.1) is not automatically closed with respect to $\langle g \rangle_f$, as there is a higher order term $\langle g \mathbf{v} \rangle_f$ present. Different closures of the moment equations lead to different hierarchies of the corresponding fluid dynamics equations. Below, we are going to look at the Euler, Navier-Stokes [4, 20, 26], Grad [21, 22] and regularized Grad [33, 34, 36] equations.

5.1. The diffusive Euler equations. It is well known (see, for example, [9, 20, 21, 26]) that the collision moments of the density, momentum and energy are zeros, due to the mass, momentum, and energy conservation during the collisions of the particles:

$$(5.3) \quad \langle 1 \rangle_{\mathcal{C}(f)} = 0, \quad \langle \mathbf{v} \rangle_{\mathcal{C}(f)} = \mathbf{0}, \quad \langle \|\mathbf{v}\|^2 \rangle_{\mathcal{C}(f)} = 0.$$

Thus, the transport equations for these moments read

$$(5.4a) \quad \frac{\partial \rho}{\partial t} + \operatorname{div} \langle \mathbf{v} \rangle_f = \operatorname{div} \left(\frac{D_\alpha}{\rho \theta} \nabla (\rho \theta) \right),$$

$$(5.4b) \quad \frac{\partial \langle \mathbf{v} \rangle_f}{\partial t} + \operatorname{div} \langle \mathbf{v} \otimes \mathbf{v} \rangle_f = \operatorname{div} \left(\frac{D_\alpha}{\rho \theta} (\nabla \otimes (\theta \langle \mathbf{v} \rangle_f)) \right),$$

$$(5.4c) \quad \frac{1}{2} \frac{\partial \langle \|v\|^2 \rangle_f}{\partial t} + \frac{1}{2} \operatorname{div} \langle \|v\|^2 v \rangle_f = \frac{1}{2} \operatorname{div} \left(\frac{D_\alpha}{\rho \theta} \nabla (\theta \langle \|v\|^2 \rangle_f) \right),$$

where the divergence of a tensor contracts over its first index. Let us define the $N \times N$ -dimensional stress matrix \mathbf{S} and the N -dimensional heat flux vector \mathbf{q} via the relations

$$(5.5) \quad \mathbf{S} = \frac{1}{\rho} \langle (v - u) \otimes (v - u) \rangle_f - \theta \mathbf{I}, \quad \mathbf{q} = \frac{1}{2\rho} \langle \|v - u\|^2 (v - u) \rangle_f.$$

Note that here the moments of the stress \mathbf{S} and heat flux \mathbf{q} are normalized by the density ρ . This is unlike the conventional notation in, for example, [21], where the stress and heat flux are given by the corresponding unnormalized moments. However, here we prefer the notations in (5.5) due to the fact that they are analogous to the velocity u and temperature θ , and thus are more suitable for defining the boundary conditions for gas flows. Indeed, observe that it is the velocity u and temperature θ which are typically specified at the boundaries, as opposed to the momentum ρu and pressure $\rho \theta$.

One then can verify directly that \mathbf{S} and \mathbf{q} satisfy the relations

$$(5.6a) \quad \langle v \otimes v \rangle_f = \rho(u \otimes u + \theta \mathbf{I} + \mathbf{S}),$$

$$(5.6b) \quad \frac{1}{2} \langle \|v\|^2 v \rangle_f = \rho \left(\frac{1}{2} \|u\|^2 u + \frac{N+2}{2} \theta u + \mathbf{S}u + \mathbf{q} \right).$$

Clearly, the equations in (5.4) above are closed with respect to ρ , u and θ , but not with respect to \mathbf{S} or \mathbf{q} . The Euler closure for (5.4) is achieved under the assumption that the particle velocity distribution f is equal to the Maxwell-Boltzmann statistical equilibrium [20, 26], given in the form

$$(5.7) \quad f_{MB} = \frac{\rho}{(2\pi\theta)^{N/2}} \exp \left(-\frac{\|v - u\|^2}{2\theta} \right),$$

which sets both the stress \mathbf{S} and heat flux \mathbf{q} to zero. Substituting zero stress and heat flux into the moment transport equations in (5.4), we obtain

$$(5.8a) \quad \frac{\partial \rho}{\partial t} + \operatorname{div}(\rho u) = \operatorname{div} \left(\frac{D_\alpha}{\rho \theta} \nabla(\rho \theta) \right),$$

$$(5.8b) \quad \frac{\partial(\rho u)}{\partial t} + \operatorname{div}(\rho(u \otimes u + \theta \mathbf{I})) = \operatorname{div} \left(\frac{D_\alpha}{\rho \theta} (\nabla \otimes (\rho \theta u)) \right),$$

$$(5.8c) \quad \frac{\partial}{\partial t} \left(\rho \left(\frac{1}{2} \|u\|^2 + \frac{N}{2} \theta \right) \right) + \operatorname{div} \left(\rho \left(\frac{1}{2} \|u\|^2 + \frac{N+2}{2} \theta \right) u \right) = \operatorname{div} \left(\frac{D_\alpha}{\rho \theta} \nabla \left(\rho \theta \left(\frac{1}{2} \|u\|^2 + \frac{N}{2} \theta \right) \right) \right).$$

Above, the x -differentiation is formally done for each degree of freedom of a gas particle (that is, 3 translational degrees, and $(N - 3)$ rotational degrees). However, in practical situations it is assumed that the moment averages are distributed uniformly along the

rotational degrees (that is, the orientation angles of particles), and thus only the translational \mathbf{x} -differentiations are often taken into account. Also, it is usually assumed that the rotational components of the momentum $\langle \mathbf{v} \rangle_f$ are zero, and thus the equations above are entirely closed with respect to the density ρ , the temperature θ , and the translational components of the velocity \mathbf{u} as functions of the translational coordinates of \mathbf{x} .

Recalling the standard expression for the adiabatic exponent

$$(5.9) \quad \gamma = 1 + \frac{2}{N},$$

one can recast the energy equation into a more conventional form

$$(5.10) \quad \frac{\partial}{\partial t} \left(\rho \left(\frac{1}{2} \|\mathbf{u}\|^2 + \frac{\theta}{\gamma - 1} \right) \right) + \operatorname{div} \left(\rho \left(\frac{1}{2} \|\mathbf{u}\|^2 \mathbf{u} + \frac{\gamma \theta \mathbf{u}}{\gamma - 1} \right) \right) = \\ = \operatorname{div} \left(\frac{D_\alpha}{\rho \theta} \nabla \left(\rho \theta \left(\frac{1}{2} \|\mathbf{u}\|^2 + \frac{\theta}{\gamma - 1} \right) \right) \right).$$

The equations in (5.8) and (5.10) above are the diffusive analogs of the well-known Euler equations [4, 20, 26]. Observe that the new diffusion term from (4.13) manifests itself in all moment equations.

One can also write the separate equation for the product $\rho \theta$ (which, for an ideal gas, constitutes the pressure). For that, observe that

$$(5.11a) \quad \frac{1}{2} \frac{\partial}{\partial t} (\rho \|\mathbf{u}\|^2) = \mathbf{u} \cdot \frac{\partial}{\partial t} (\rho \mathbf{u}) - \frac{1}{2} \|\mathbf{u}\|^2 \frac{\partial \rho}{\partial t},$$

$$(5.11b) \quad \frac{1}{2} \operatorname{div} (\rho \|\mathbf{u}\|^2 \mathbf{u}) = \mathbf{u} \cdot \operatorname{div} (\rho \mathbf{u} \otimes \mathbf{u}) - \frac{1}{2} \|\mathbf{u}\|^2 \operatorname{div} (\rho \mathbf{u}),$$

$$(5.11c) \quad \frac{1}{2} \operatorname{div} \left(\frac{D_\alpha}{\rho \theta} \nabla (\rho \theta \|\mathbf{u}\|^2) \right) = \mathbf{u} \cdot \operatorname{div} \left(\frac{D_\alpha}{\rho \theta} (\nabla \otimes (\rho \theta \mathbf{u})) \right) - \\ - \frac{1}{2} \|\mathbf{u}\|^2 \operatorname{div} \left(\frac{D_\alpha}{\rho \theta} \nabla (\rho \theta) \right) + D_\alpha \|\nabla \otimes \mathbf{u}\|^2,$$

and thus, subtracting the appropriate multiples of the density and momentum equations, we obtain

$$(5.12) \quad \frac{\partial (\rho \theta)}{\partial t} + \operatorname{div} (\rho \theta \mathbf{u}) + (\gamma - 1) \rho \theta \operatorname{div} \mathbf{u} = \operatorname{div} \left(\frac{D_\alpha}{\rho \theta} \nabla (\rho \theta^2) \right) + (\gamma - 1) D_\alpha \|\nabla \otimes \mathbf{u}\|^2.$$

Above, $\|\nabla \otimes \mathbf{u}\|^2$ is given by

$$(5.13) \quad \|\nabla \otimes \mathbf{u}\|^2 = (\nabla \otimes \mathbf{u}) : (\nabla \otimes \mathbf{u}),$$

where “:” denotes the Frobenius product of two matrices. Observe that the diffusive Euler equations above are of the second order in \mathbf{x} , and thus are more suitable for a Dirichlet boundary value problem, than the conventional Euler equations (which are of the first order in \mathbf{x}).

5.2. The diffusive Navier-Stokes equations. The conventional Navier-Stokes equations [4, 20, 26] are obtained as an “upgrade” from the conventional Euler equations by approximating the stress \mathbf{S} and heat flux \mathbf{q} in (5.6) via the Newton and Fourier laws, under the assumption that the dynamics of the stress and heat flux manifests itself on a much faster time scale and is thus “slaved” to the slower dynamics of the density, momentum and energy. The Newton law for the stress \mathbf{S} and the Fourier law for the heat flux \mathbf{q} are given, respectively, by

$$(5.14a) \quad \mathbf{S}_{Newton} = -\frac{\mu}{\rho} \left(\nabla \otimes \mathbf{u} + (\nabla \otimes \mathbf{u})^T + (1 - \gamma)(\operatorname{div} \mathbf{u}) \mathbf{I} \right),$$

$$(5.14b) \quad \mathbf{q}_{Fourier} = -\frac{1}{Pr} \frac{\gamma}{\gamma - 1} \frac{\mu}{\rho} \nabla \theta,$$

where μ is the dynamic viscosity and Pr is the Prandtl number. Here we obtain the diffusive Navier-Stokes equations from the diffusive Euler equations in (5.8) in exactly the same manner, by substituting the Newton and Fourier laws in (5.14) into the moment expressions in (5.6):

$$(5.15a) \quad \frac{\partial \rho}{\partial t} + \operatorname{div}(\rho \mathbf{u}) = \operatorname{div} \left(\frac{D_\alpha}{\rho \theta} \nabla(\rho \theta) \right),$$

$$(5.15b) \quad \frac{\partial(\rho \mathbf{u})}{\partial t} + \operatorname{div}(\rho \mathbf{u} \otimes \mathbf{u}) + \nabla(\rho \theta) = \operatorname{div} \left(\frac{D_\alpha}{\rho \theta} \left(\nabla \otimes (\rho \theta \mathbf{u}) \right) \right) + \\ + \operatorname{div} \left(\mu \left(\nabla \otimes \mathbf{u} + (\nabla \otimes \mathbf{u})^T \right) \right) + (1 - \gamma) \nabla(\mu \operatorname{div} \mathbf{u}),$$

$$(5.15c) \quad \frac{\partial(\rho \theta)}{\partial t} + \operatorname{div}(\rho \theta \mathbf{u}) + (\gamma - 1) \rho \theta \operatorname{div} \mathbf{u} = \operatorname{div} \left(\frac{D_\alpha}{\rho \theta} \nabla(\rho \theta^2) \right) + \frac{\gamma}{Pr} \operatorname{div}(\mu \nabla \theta) + \\ + (\gamma - 1) \left((D_\alpha + \mu) \|\nabla \otimes \mathbf{u}\|^2 + \mu \left((\nabla \otimes \mathbf{u}) : (\nabla \otimes \mathbf{u})^T + (1 - \gamma)(\operatorname{div} \mathbf{u})^2 \right) \right).$$

The diffusive Navier-Stokes equations above are somewhat similar to those in the works on the extended fluid dynamics [6–8, 14, 15, 17]. Above, the dependence of the dynamic viscosity μ on the temperature is approximated in the same manner as for the dynamic mass diffusivity:

$$(5.16) \quad \mu = \mu^* \sqrt{\frac{\theta}{\theta^*}},$$

where μ^* is the reference viscosity for a reference temperature θ^* . Note that Sutherland’s law [35] provides a more precise dependence of the viscosity on the temperature, however, the simplified relation in (5.16) suffices for our purposes in this work.

The reduction of the phase space to the translational components of the velocity \mathbf{u} in (5.15) is done in the same way as for the Euler equations above – by assuming that the rotational components of \mathbf{u} are zero, and that the spatial derivatives of all variables in rotational dimensions are also zero.

5.3. The diffusive Grad equations. For the diffusive Grad equations, we augment the existing transport equations in (5.4) with the new transport equations for the stress and heat flux moments, given by

$$(5.17a) \quad \frac{\partial \langle \mathbf{v} \otimes \mathbf{v} \rangle_f}{\partial t} + \operatorname{div} \langle \mathbf{v} \otimes \mathbf{v} \otimes \mathbf{v} \rangle_f = \langle \mathbf{v} \otimes \mathbf{v} \rangle_{\mathcal{C}(f)} + \operatorname{div} \left(\frac{D_\alpha}{\rho \theta} \left(\nabla \otimes (\theta \langle \mathbf{v} \otimes \mathbf{v} \rangle_f) \right) \right),$$

$$(5.17b) \quad \frac{1}{2} \frac{\partial \langle \|\mathbf{v}\|^2 \mathbf{v} \rangle_f}{\partial t} + \frac{1}{2} \operatorname{div} \langle \|\mathbf{v}\|^2 \mathbf{v} \otimes \mathbf{v} \rangle_f = \frac{1}{2} \langle \|\mathbf{v}\|^2 \mathbf{v} \rangle_{\mathcal{C}(f)} + \frac{1}{2} \operatorname{div} \left(\frac{D_\alpha}{\rho \theta} \left(\nabla \otimes (\theta \langle \|\mathbf{v}\|^2 \mathbf{v} \rangle_f) \right) \right).$$

Observe that the collision terms are nonzero for the stress \mathbf{S} and heat flux \mathbf{q} (as opposed to the density, momentum and energy). Also, the new equations include the unknown higher-order moments $\langle \mathbf{v} \otimes \mathbf{v} \otimes \mathbf{v} \rangle_f$ and $\langle \|\mathbf{v}\|^2 \mathbf{v} \otimes \mathbf{v} \rangle_f$. For these higher-order moments, we introduce the corresponding centered moments

$$(5.18) \quad \mathbf{Q} = \frac{1}{\rho} \langle (\mathbf{v} - \mathbf{u}) \otimes (\mathbf{v} - \mathbf{u}) \otimes (\mathbf{v} - \mathbf{u}) \rangle_f, \quad \mathbf{R} = \frac{1}{2\rho} \langle \|\mathbf{v} - \mathbf{u}\|^2 (\mathbf{v} - \mathbf{u}) \otimes (\mathbf{v} - \mathbf{u}) \rangle_f,$$

with \mathbf{Q} being the $N \times N \times N$ 3-rank tensor, and \mathbf{R} being the $N \times N$ matrix. One can verify that \mathbf{Q} and \mathbf{R} satisfy the identities

$$(5.19a) \quad \frac{1}{\rho} \langle \mathbf{v} \otimes \mathbf{v} \otimes \mathbf{v} \rangle_f = \mathbf{u} \otimes \mathbf{u} \otimes \mathbf{u} + (\theta \mathbf{I} + \mathbf{S}) \otimes \mathbf{u} + ((\theta \mathbf{I} + \mathbf{S}) \otimes \mathbf{u})^T + ((\theta \mathbf{I} + \mathbf{S}) \otimes \mathbf{u})^{TT} + \mathbf{Q},$$

$$(5.19b) \quad \frac{1}{2\rho} \langle \|\mathbf{v}\|^2 \mathbf{v} \otimes \mathbf{v} \rangle_f = \frac{1}{2} \|\mathbf{u}\|^2 \mathbf{u} \otimes \mathbf{u} + \frac{2\gamma - 1}{\gamma - 1} \theta \mathbf{u} \otimes \mathbf{u} + \frac{1}{2} \|\mathbf{u}\|^2 (\theta \mathbf{I} + \mathbf{S}) + (\mathbf{S} \mathbf{u} + \mathbf{q}) \otimes \mathbf{u} + \mathbf{u} \otimes (\mathbf{S} \mathbf{u} + \mathbf{q}) + \mathbf{Q} \mathbf{u} + \mathbf{R},$$

where “ TT ” denotes the double transposition of a 3-rank tensor. In order to approximate the higher-order centered moments \mathbf{Q} and \mathbf{R} , we use the Grad distribution [21]

$$(5.20) \quad f_{\text{Grad}} = f_{\text{MB}} \left(1 + \frac{1}{2\theta^2} (\mathbf{v} - \mathbf{u})^T \mathbf{S} (\mathbf{v} - \mathbf{u}) + \frac{1}{\theta^2} \left(\frac{\gamma - 1}{2\gamma\theta} \|\mathbf{v} - \mathbf{u}\|^2 - 1 \right) \mathbf{q} \cdot (\mathbf{v} - \mathbf{u}) \right),$$

which is chosen so as to satisfy the prescribed ρ , \mathbf{u} , θ , \mathbf{S} and \mathbf{q} . For the derivation of f_{Grad} for a polyatomic gas particle, see, for example, [27]. For the higher-order moments \mathbf{Q} and \mathbf{R} we use their Grad approximations, provided by f_{Grad} :

$$(5.21a) \quad \mathbf{Q}_{\text{Grad}} = \frac{\gamma - 1}{\gamma} \left(\mathbf{I} \otimes \mathbf{q} + (\mathbf{I} \otimes \mathbf{q})^T + (\mathbf{I} \otimes \mathbf{q})^{TT} \right),$$

$$(5.21b) \quad \mathbf{R}_{\text{Grad}} = \frac{\gamma}{\gamma - 1} \theta^2 \mathbf{I} + \frac{2\gamma - 1}{\gamma - 1} \theta \mathbf{S}.$$

Substituting the approximations above into the moment relations, we obtain

$$(5.22a) \quad \frac{1}{\rho} \langle \mathbf{v} \otimes \mathbf{v} \otimes \mathbf{v} \rangle_{f_{Grad}} = \mathbf{u} \otimes \mathbf{u} \otimes \mathbf{u} + (\theta \mathbf{I} + \mathbf{S}) \otimes \mathbf{u} + ((\theta \mathbf{I} + \mathbf{S}) \otimes \mathbf{u})^T + \\ + ((\theta \mathbf{I} + \mathbf{S}) \otimes \mathbf{u})^{TT} + \frac{\gamma - 1}{\gamma} \left(\mathbf{I} \otimes \mathbf{q} + (\mathbf{I} \otimes \mathbf{q})^T + (\mathbf{I} \otimes \mathbf{q})^{TT} \right),$$

$$(5.22b) \quad \frac{1}{2\rho} \langle \|\mathbf{v}\|^2 \mathbf{v} \otimes \mathbf{v} \rangle_{f_{Grad}} = \left(\frac{1}{2} \|\mathbf{u}\|^2 + \frac{2\gamma - 1}{\gamma - 1} \theta \right) (\mathbf{u} \otimes \mathbf{u} + \mathbf{S}) + \left(\frac{1}{2} \theta \|\mathbf{u}\|^2 + \right. \\ \left. + \frac{\gamma}{\gamma - 1} \theta^2 + \frac{\gamma - 1}{\gamma} (\mathbf{q} \cdot \mathbf{u}) \right) \mathbf{I} + \left(\mathbf{S} \mathbf{u} + \frac{2\gamma - 1}{\gamma} \mathbf{q} \right) \otimes \mathbf{u} + \mathbf{u} \otimes \left(\mathbf{S} \mathbf{u} + \frac{2\gamma - 1}{\gamma} \mathbf{q} \right).$$

As in [21], we approximate the moment collision terms via the linear damping:

$$(5.23) \quad \langle \mathbf{v} \otimes \mathbf{v} \rangle_{\mathcal{C}(f)} = -\frac{\rho^2 \theta}{\mu} \mathbf{S}, \quad \frac{1}{2} \langle \|\mathbf{v}\|^2 \mathbf{v} \rangle_{\mathcal{C}(f)} = -\frac{\rho^2 \theta}{\mu} (\mathbf{S} \mathbf{u} + Pr \mathbf{q}).$$

As a result, the diffusive Grad equations in (5.4) and (5.17) become closed with respect to the variables ρ , \mathbf{u} , θ , \mathbf{S} and \mathbf{q} , via (4.5), (5.6), (5.22) and (5.23). Observe that the diffusive Grad equations in (5.4) and (5.17) are of the second order in x , and thus are well posed for a Dirichlet boundary value problem (unlike the original Grad equations [21, 22]).

For the reduction of the phase space to the translational components of the velocity \mathbf{u} , stress \mathbf{S} and heat flux \mathbf{q} above in the diffusive Grad equations (5.4) and (5.17) one has to assume that the rotational components of the velocity \mathbf{u} heat flux \mathbf{q} are zero, and that the spatial derivatives in the rotational directions are zero. No assumptions need to be made about the rotational components of the stress matrix, since they become decoupled from the translational transport equations. Also, observe that if no rotational components of the phase space are present (for example, if the gas is monatomic, and the physical space is fully three-dimensional), then one of the diagonal stress transport equations becomes redundant, due to the fact that the trace of \mathbf{S} is, by construction, zero.

5.4. The diffusive regularized Grad equations. Similar to the Navier-Stokes modification (5.15) of the Euler equations (5.8) via the Newton and Fourier laws (5.14), the higher-order regularization of the Grad equations in (5.4) and (5.17) was suggested in [33, 34, 36] for a monatomic gas. Here we extend the regularization of the Grad equations onto the polyatomic case and the diffusive setting, by following the same approach as in [33, 34, 36]. We present the regularization formulas for the polyatomic Grad equations while omitting their derivation, due to the excessive complexity and lengthiness of the latter.

The diffusive regularized Grad equations for a polyatomic gas are obtained directly from the diffusive Grad equations in (5.4) and (5.17) by replacing the Grad approximations for the third- and fourth-order moments \mathbf{Q}_{Grad} and \mathbf{R}_{Grad} with the regularized approximations. The expressions for the third order moment \mathbf{Q} and the fourth order moment \mathbf{R} in the regularized Grad equations are given by

$$(5.24a) \quad \mathbf{Q}_{Reg.Grad} = \mathbf{Q}_{Grad} + \tilde{\mathbf{Q}} + \tilde{\mathbf{Q}}^T + \tilde{\mathbf{Q}}^{TT},$$

$$(5.24b) \quad \mathbf{R}_{Reg, Grad} = \mathbf{R}_{Grad} + \tilde{\mathbf{R}} + \tilde{\mathbf{R}}^T + \left(\tilde{R} + (1 - \gamma) \text{tr}(\tilde{\mathbf{R}}) \right) \mathbf{I},$$

where the corrections $\tilde{\mathbf{Q}}$, \tilde{R} and $\tilde{\mathbf{R}}$ read

$$(5.25a) \quad \tilde{\mathbf{Q}} = -\frac{1}{Pr_{\tilde{\mathbf{Q}}}\rho} \left[\nabla \otimes \mathbf{S} - \frac{\gamma-1}{\gamma} \mathbf{I} \otimes \text{div} \mathbf{S} - \frac{1}{\rho\theta} \left(\mathbf{S} \otimes \text{div}(\rho \mathbf{S}) - \frac{\gamma-1}{\gamma} \mathbf{I} \otimes \mathbf{S} \text{div}(\rho \mathbf{S}) \right) + \right. \\ \left. + \frac{\gamma-1}{\gamma\theta} \left(\mathbf{q} \otimes (\nabla \otimes \mathbf{u} + (\nabla \otimes \mathbf{u})^T) - \frac{\gamma-1}{\gamma} \mathbf{I} \otimes (\nabla \otimes \mathbf{u} + (\nabla \otimes \mathbf{u})^T + (\text{div} \mathbf{u}) \mathbf{I}) \mathbf{q} \right) \right],$$

$$(5.25b) \quad \tilde{R} = -\frac{2}{Pr_{\tilde{R}}\rho} \left[\frac{\gamma}{\theta} \text{div}(\theta \mathbf{q}) - \text{div} \mathbf{q} + (\gamma-1) \left(\mathbf{S} : (\nabla \otimes \mathbf{u}) - \frac{1}{\rho\theta} \mathbf{q} \cdot \text{div}(\rho \mathbf{S}) \right) \right],$$

$$(5.25c) \quad \tilde{\mathbf{R}} = -\frac{1}{Pr_{\tilde{\mathbf{R}}}\rho} \left[\mathbf{S} (\nabla \otimes \mathbf{u} + (\nabla \otimes \mathbf{u})^T) + \frac{2\gamma-1}{\gamma\theta} \left(\nabla \otimes (\theta \mathbf{q}) - \frac{1}{\rho} \mathbf{q} \otimes \text{div}(\rho \mathbf{S}) \right) - \right. \\ \left. - \left((\gamma-1) \text{div} \mathbf{u} + \frac{2\gamma-1}{2\theta} \left(\frac{1}{\rho} \text{div}(\rho \mathbf{q}) + \mathbf{S} : (\nabla \otimes \mathbf{u}) \right) \right) \mathbf{S} \right].$$

Above, the constants $Pr_{\tilde{\mathbf{Q}}}$, $Pr_{\tilde{R}}$ and $Pr_{\tilde{\mathbf{R}}}$ are the third- and fourth-moment Prandtl numbers, which equal $3/2$, $2/3$ and $7/6$, respectively, for an ideal monatomic gas [33, 34, 36]. Unfortunately, it does not seem to be possible to compute the exact values for $Pr_{\tilde{\mathbf{Q}}}$, $Pr_{\tilde{R}}$ and $Pr_{\tilde{\mathbf{R}}}$ for a polyatomic gas in general, since the collision between polyatomic gas molecules is a complex process which depends on the fine structure of a gas molecule. It might be possible, however, to measure the values of $Pr_{\tilde{\mathbf{Q}}}$, $Pr_{\tilde{R}}$ and $Pr_{\tilde{\mathbf{R}}}$ experimentally for common polyatomic gases. In the current work, we leave the values of $Pr_{\tilde{\mathbf{Q}}}$, $Pr_{\tilde{R}}$ and $Pr_{\tilde{\mathbf{R}}}$ for nitrogen at the same values as for an ideal monatomic gas, since the experimental Prandtl number of nitrogen (~ 0.69) is not much different from the one of an ideal monatomic gas ($2/3$), and the computational results do not seem to be affected much by such a crude approximation.

6. A SIMPLE COMPUTATIONAL TEST: THE COUETTE FLOW

The Couette flow is a simplest form of a two-dimensional gas flow between two infinite moving parallel walls. It is assumed that the gas “sticks” to the walls to some extent, such that the velocity \mathbf{u} of the flow assumes different values at the boundaries (due to the walls moving with different speeds relative to each other). Despite its simplicity, the Couette flow problem is not well-posed for the conventional Euler or Grad equations, since both are the first-order differential equations in the space variable \mathbf{x} , and thus become overdetermined in the case of different Dirichlet boundary conditions at different walls. Instead, conventionally the Couette flow problem is solved via the famous Navier-Stokes equations [4, 20, 26], which, in our case, can be obtained directly from the diffusive Navier-Stokes equations in (5.15) by setting the scaled mass diffusivity $D_\alpha = 0$. Conventionally, the Navier-Stokes equations are obtained from the hierarchy of the moment transport equations by the Chapman-Enskog perturbation expansion [13, 20, 26],

with the Newton and Fourier laws used to express the stress and heat flux. Observe that the Navier-Stokes equations in (5.15) are of the second order in the momentum and energy, even if the scaled mass diffusivity D_α is set to zero. This allows to specify the velocity and temperature at both walls without making the problem overdetermined.

On the other hand, the diffusive Boltzmann equation in (4.13) is already of the second order in x , and so become all its moment equations, including the diffusive Euler (5.8) and Grad (5.4), (5.17) equations. This makes these equations naturally suitable for a Dirichlet boundary value problem, and, in particular, the Couette flow, without having to resort to the the Fourier and Newton laws for the stress and heat flux. In this work, we compute the Couette flow for the conventional Navier-Stokes, diffusive Euler, diffusive Navier-Stokes, diffusive Grad and regularized diffusive Grad equations, and compare the results to the Direct Simulation Monte Carlo method.

6.1. The Direct Simulation Monte Carlo method. The Direct Simulation Monte Carlo (DSMC) method [5] is a “brute force” method to compute stationary gas flows by simulating the random motion and collisions of the actual gas particles (thus the title of the method). Due to the detailed particle interpretation of the gas, the DSMC method allows great versatility of the particle collision dynamics, including the ability to simulate the collisions of polyatomic gas molecules, and also the mixtures of different gases. The main practical downside of the DSMC method is its tremendous computational expense, as opposed to the fluid dynamics approach. We use the DSMC results of the Couette flow simulation as the “true” benchmark flow to compare other results against. For the numerical computation of the DSMC, we use the DS1V software, written by Prof. G.A. Bird and available for download on his website¹. For the purposes of this work, we modified the DS1V code to compute and output the stress and heat flux of the flow inside the domain, in addition to the density, velocity and temperature (the original DS1V code outputs the cross-stress and normal heat flux at the boundaries only).

6.2. Details of the numerical implementation. For the Couette flow, the standard assumption is that the flow is “1.5-dimensional”. More precisely, let us denote the direction from one wall to the other as x -direction, the direction of the gas flow as y -direction, so that the z -direction is the one orthogonal to both. Then, the following assumptions are made:

- **z -coordinate.** The z -coordinate is treated precisely in the same manner as a rotational degree of freedom. In particular, it is assumed that the z -components of the velocity and heat flux are zero, and that the z -derivatives of all flow variables are zero.
- **y -coordinate.** It is assumed that the y -derivatives of all flow variables are identically zero. It is, however, not assumed that the y -components of vector- and tensor-variables are necessarily zero.

The spatial discretization scheme utilizes second-order centered differences of the flux components for each moment variable in (5.4) and (5.17), which is a standard approach for modeling flows. This allows to preserve the spatial integral of a moment variable

¹<http://gab.com.au>

exactly, as long as the collision damping or the boundary conditions do not interfere. In the current set-up, only the integral of the density ρ is preserved exactly, since such preservation for the momentum and energy is precluded by the Dirichlet boundary conditions on the velocity and temperature, while the stress and heat flux are affected by the collision damping. The standard 4th-order Runge-Kutta scheme is used to integrate the model equations forward in time.

6.3. The Couette flow for argon. Argon is a monatomic gas, with observed kinetic behavior very close to the ideal gas theory predictions ($\gamma = 5/3$, $Pr = 2/3$). The DSMC computational set-up for the Couette flow for argon was as follows:

- Distance between the walls: 10^{-6} meters;
- Difference in wall velocities: 100 meters per second;
- Temperature of each wall: 288.15 K (15° Celsius);
- Average number density of argon: $2.5 \cdot 10^{25}$ particles per cubic meter, which corresponds to the argon density $\rho = 1.658$ kilogram per cubic meter. This number density is chosen so that the number of particles is similar to that in the Earth atmosphere at sea level.

Due to slipping, the actual values of the thermodynamic quantities at the boundaries were the following:

- Actual difference in the parallel velocity of the flow at the boundaries: 90.25 meters per second;
- Actual temperature of the flow at each boundary: 288.7 K.

For all fluid dynamics equations we used the following expressions for the viscosity μ and the scaled mass diffusivity D_α :

$$(6.1) \quad \mu = \mu^* \sqrt{\frac{M\theta}{RT^*}}, \quad D_\alpha = D_\alpha^* \sqrt{\frac{M\theta}{RT^*}},$$

where $R = 8.314 \text{ kg m}^2/(\text{mol K sec}^2)$ is the universal gas constant, M is the molar mass of the gas ($3.995 \cdot 10^{-2} \text{ kg/mol}$ for argon), $T^* = 288.15 \text{ K}$ (that is, 15° C), and the reference constants μ^* and D_α^* were chosen as follows:

- The reference viscosity μ^* was set to the standard reference value $2.2 \cdot 10^{-5} \text{ kg}/(\text{m sec})$ at 15° C for argon [25].
- The reference mass diffusion coefficient D_α^* was chosen so that the diffusive Euler equations for the Couette flow produced a good correspondence with the DSMC simulation (we found via a few trials that $D_\alpha^* = 4 \cdot 10^{-6} \text{ kg}/(\text{m sec})$ produces a good match).

We then carried out the numerical simulations with both the conventional Navier-Stokes, diffusive Euler and diffusive Navier-Stokes equations until a steady solution was reached, which we found to occur in about $3 \cdot 10^{-8}$ seconds. The density, temperature and y -velocity profiles, corresponding to the conventional Navier-Stokes, the diffusive Euler equations, and the diffusive Navier-Stokes equations are compared with the DSMC profiles on Figure 1. Observe that the density and temperature profiles are captured rather

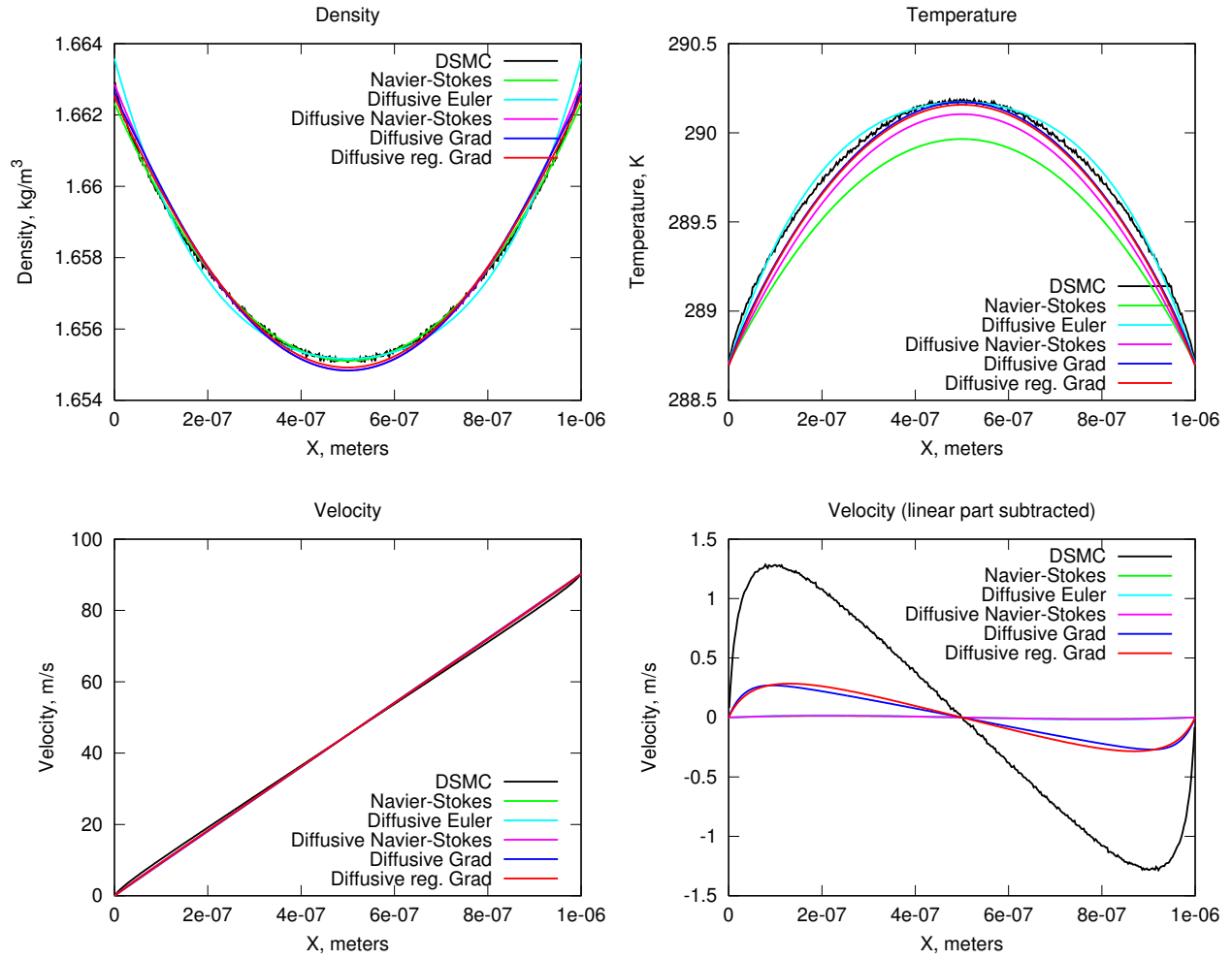


FIGURE 1. The density, velocity and temperature of the Couette flow for argon.

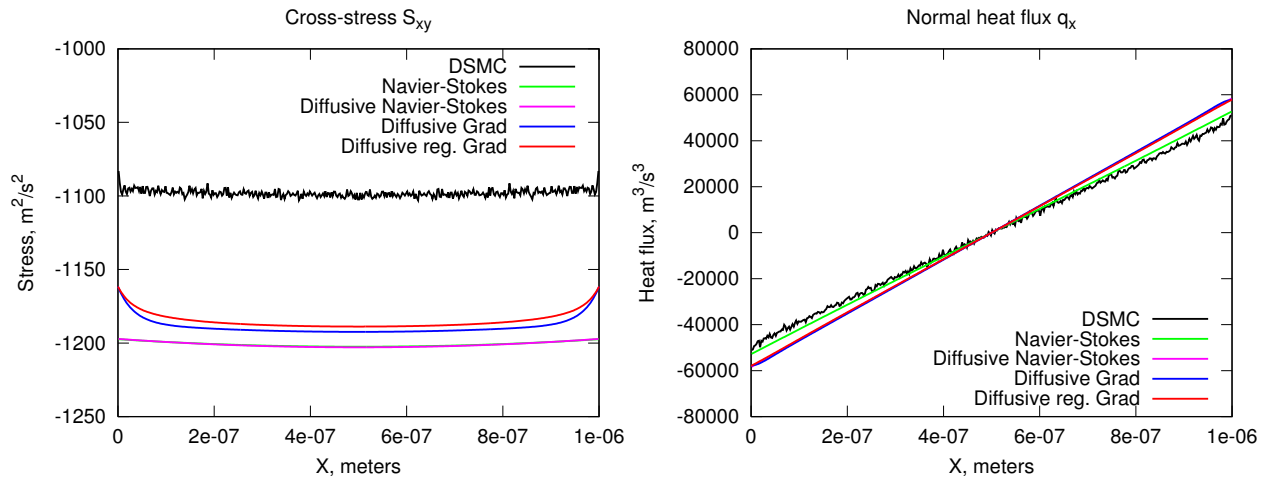


FIGURE 2. The cross-stress and normal heat flux for the Couette flow for argon.

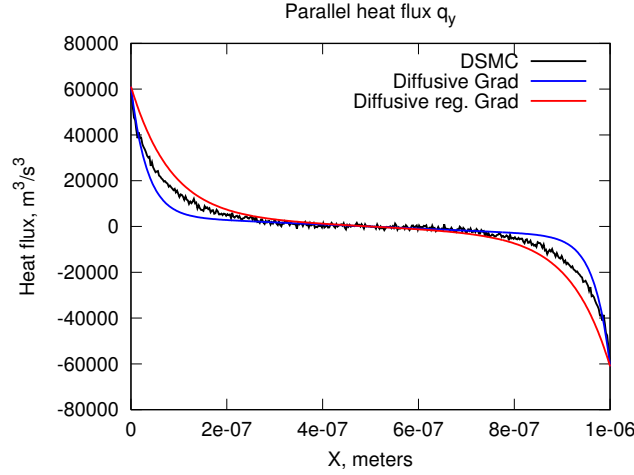


FIGURE 3. The parallel heat flux for the Couette flow for argon.

well by both the conventional and diffusive Navier-Stokes equations, as well as the diffusive Euler equations. However, the DSMC velocity profiles clearly exhibit the Knudsen boundary layers, which neither the Navier-Stokes (either conventional or diffusive) nor the diffusive Euler equations were able to capture.

For the diffusive Grad and the regularized diffusive Grad equations we chose the following parameters. First, we set $\mu = 2.2 \cdot 10^{-5}$ kg/(m sec), and $D_\alpha = 4 \cdot 10^{-6}$ kg/(m sec), as above for the diffusive Navier-Stokes equations. Second, we set the diagonal components of the stress, S_{xx} and S_{yy} , to zero at the boundaries. The value of the cross-stress component S_{xy} was set to $-1.161 \cdot 10^3$ m²/s² at both boundaries, as was measured in the DSMC simulations by the DS1V program. The value of the normal heat flux component q_x was set to $\pm 5.792 \cdot 10^4$ m³/s³ at both boundaries (negative value on the left boundary, and positive value on the right boundary), as was also reported by the DS1V program. We set the value of the parallel heat flux component q_y to $\pm 6.113 \cdot 10^4$ m³/s³ at the boundaries as reported by the DS1V program (positive value on the left boundary, and negative value on the right boundary).

The results of the simulation with the diffusive Grad and the regularized diffusive Grad equations are also shown in Figure 1. Observe that, in addition to the reasonably well-captured density and temperature profiles, the diffusive Grad and the regularized diffusive Grad equations also exhibit the weak Knudsen-like boundary layers for the y -velocity of the flow, similar to those produced by the DSMC.

In Figure 2 we show the components of the stress and heat flux for the DSMC simulations, the Navier-Stokes equations (both conventional and diffusive), and both the diffusive and regularized diffusive Grad equations. For both the conventional and diffusive Navier-Stokes equations, the cross-stress component S_{xy} and normal heat flux component q_x were computed from the corresponding Newton and Fourier laws in (5.14). We do not show that diagonal components of the stress S_{xx} and S_{yy} , since they are quite small (about two orders of magnitude smaller than the cross-stress S_{xy} , and roughly four orders of magnitude smaller than the temperature).

Observe that for the cross-stress S_{xy} the results from the Navier-Stokes and Grad closures are quite similar, while the DSMC output (which was implemented by us in the DS1V program) is somewhat different, by about 10%. What is also surprising, is that the DSMC boundary values for both the cross-stress S_{xy} and normal heat flux q_x , computed by the original DS1V routines, and used as the boundary conditions for the diffusive and regularized diffusive Grad equations, are much closer to the values of S_{xy} and q_x inside the domain as produced by the Navier-Stokes and Grad closures, while differing somewhat from what our modification of the DS1V program computes for S_{xy} and q_x inside the domain. It is possible that our modification of the DS1V program to output the cross-stress inside the domain is not quite correct, and an additional testing against a different DSMC implementation, which outputs the values of the cross-stress S_{xy} and normal heat flux q_x inside the domain by default, is needed.

In Figure 3 we show the parallel component q_y of the heat flux for the DSMC simulation, as well as for the both conventional and regularized diffusive Grad approximations. The surprising observation here is that the magnitude of the parallel heat flux q_y is of the same order of magnitude as the normal heat flux q_x , despite the fact that both the conventional and diffusive Navier-Stokes closures are quite adept at capturing q_x and at the same time are completely “unaware” of q_y . At the same time, both the diffusive and regularized diffusive Grad closures capture the parallel heat flux qualitatively well, with some quantitative discrepancies. This suggests that for practical applications where the heat fluxes are important (such as the Earth atmosphere modeling, for example), one should consider the Grad closures as a better alternative to the Navier-Stokes closures.

6.4. The Couette flow for nitrogen. The DSMC computational set-up for the Couette flow for nitrogen was largely the same as previously for argon:

- Distance between the walls: 10^{-6} meters;
- Difference in wall velocities: 100 meters per second;
- Temperature of each wall: 288.15 K (15° Celsius);
- Average number density of nitrogen: $2.5 \cdot 10^{25}$ particles per cubic meter (which corresponds to the nitrogen density $\rho = 1.163$ kilogram per cubic meter).

Due to slipping, the actual values of the thermodynamic quantities at the boundaries were the following:

- Actual difference in the parallel velocity of the flow at the boundaries: 90.78 meters per second;
- Actual temperature of the flow at each boundary: 288.4 K.

For the Navier-Stokes (both conventional and diffusive) and diffusive Euler equations we used the same expressions for the viscosity μ and the scaled mass diffusivity coefficient D_α as in (6.1) with the same reference diffusivity constant $D_\alpha^* = 4 \cdot 10^{-6}$ kg/(m sec), however, the molar mass M was replaced with that of nitrogen (that is, $2.801 \cdot 10^{-2}$ kg/mol) and the reference viscosity constant was set to $1.74 \cdot 10^{-5}$ kg/(m sec), which is a standard value for nitrogen at 15° C [25]. The Prandtl number was set to $Pr = 0.69$ (also a standard value for nitrogen at 15° C). We then carried out numerical simulations with both the conventional and diffusive Navier-Stokes equations, and the diffusive Euler equations, until a steady solution was reached (also about $3 \cdot 10^{-8}$ seconds). The

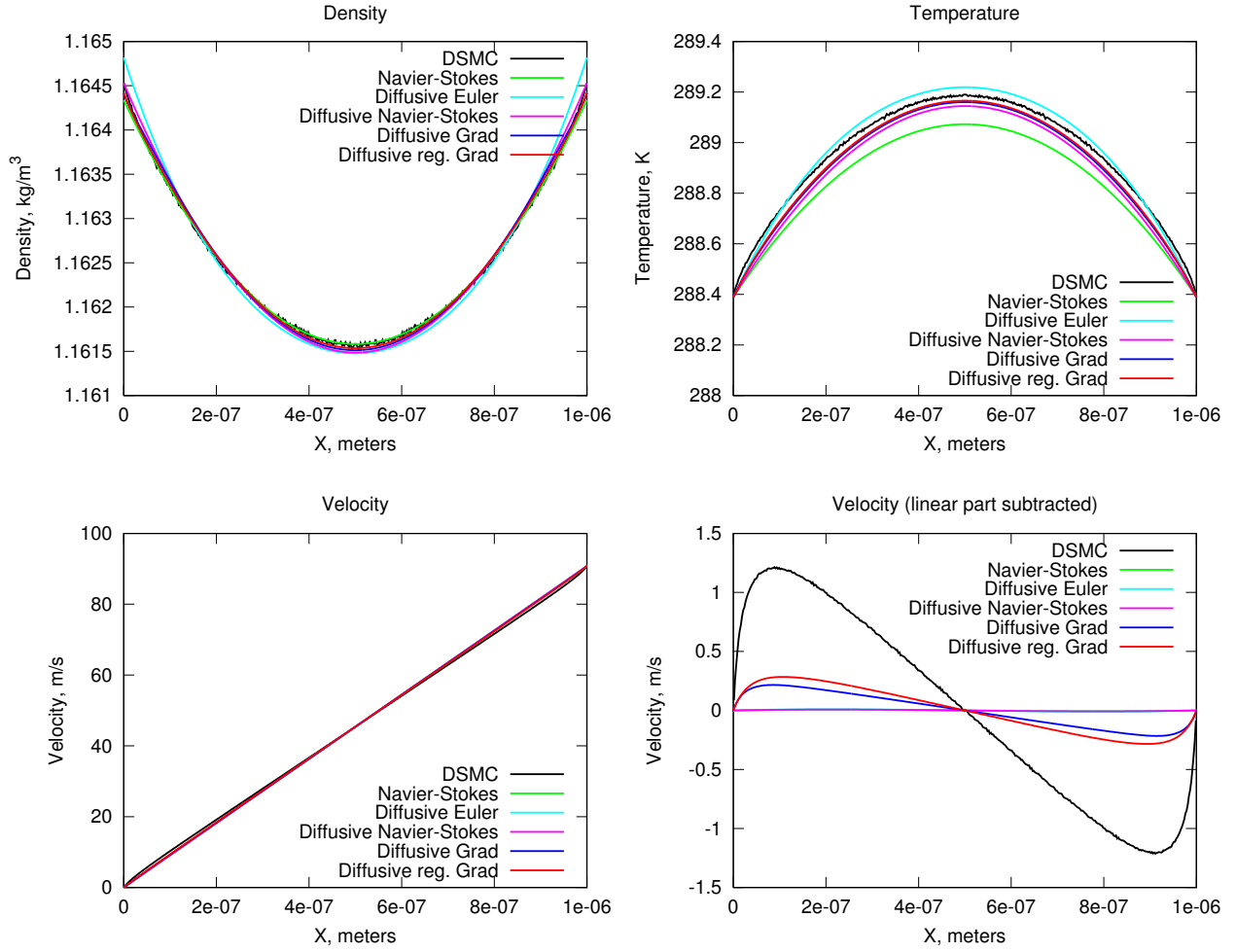


FIGURE 4. The density, velocity and temperature of the Couette flow for nitrogen.

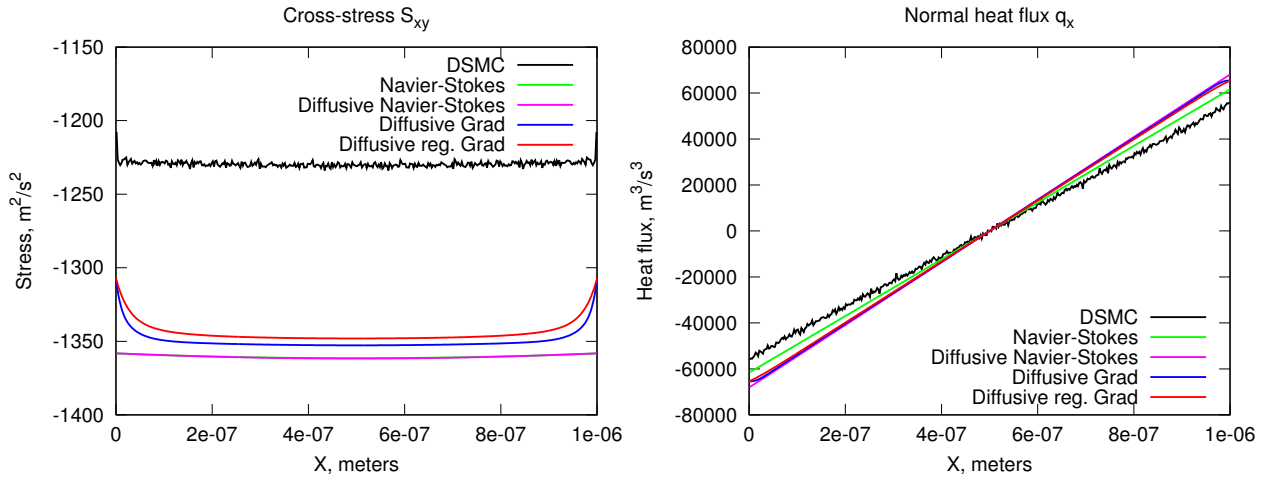


FIGURE 5. The cross-stress and normal heat flux for the Couette flow for nitrogen.

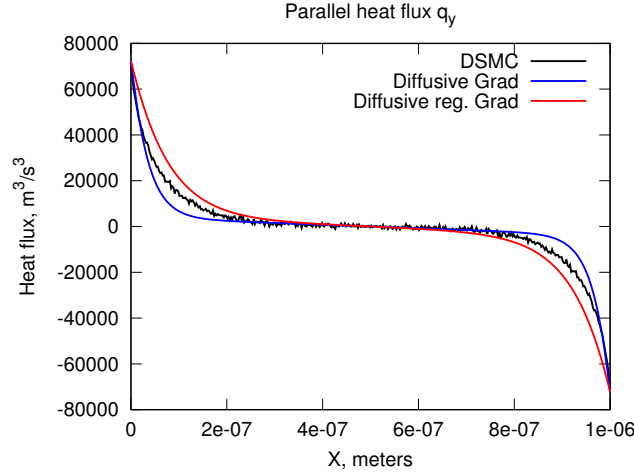


FIGURE 6. The parallel heat flux for the Couette flow for nitrogen.

density, temperature and y -velocity profiles, corresponding to both the conventional and diffusive Navier-Stokes equations, and the diffusive Euler equations, are compared with the DSMC profiles on Figure 4. Again, observe that the density and temperature profiles are captured rather well by either the Navier-Stokes (both conventional and diffusive) or the diffusive Euler equations. However, just as for argon, the DSMC velocity profiles clearly exhibit the Knudsen boundary layers, which neither the Navier-Stokes nor the diffusive Euler equations were able to capture.

For the diffusive and the regularized diffusive Grad equations we chose the following parameters. First, we set $\mu = 1.74 \cdot 10^{-5}$ kg/(m sec), and $D_\alpha = 4 \cdot 10^{-6}$ kg/(m sec), as above for the diffusive Navier-Stokes equations. Second, due to the fact that the Prandtl number for nitrogen is not much different from the Prandtl number of a monatomic ideal gas, we left the values of the third- and fourth-moment Prandtl numbers, $Pr_{\tilde{Q}}$, $Pr_{\tilde{R}}$ and $Pr_{\tilde{R}}$ at their values for a monatomic gas, $3/2$, $2/3$ and $7/6$, respectively [33, 34, 36]. Also, we set the diagonal components of the stress, S_{xx} and S_{yy} , to zero at the boundaries. The value of the cross-stress component S_{xy} was set to $-1.307 \cdot 10^3$ m²/s² at both boundaries, as was measured in the DSMC simulations by the DS1V program. The value of the normal heat flux component q_x was set to $\pm 6.541 \cdot 10^4$ m³/s³ at both boundaries (negative value on the left boundary, and positive value on the right boundary), as was also reported by the DS1V program. We set the value of the parallel heat flux component q_y to $\pm 7.228 \cdot 10^4$ m³/s³ at the boundaries as reported by the DS1V program (positive value on the left boundary, and negative value on the right boundary). The results are shown in Figure 4. Surprisingly, this simplified treatment of the air still produces qualitatively matching results, namely, the weak Knudsen-like boundary layers for the velocity manifest themselves in the diffusive and regularized diffusive Grad equations in similar way as above for argon.

In Figure 5 we show the components of the stress and heat flux for the DSMC simulations, the Navier-Stokes equations (both conventional and diffusive), the diffusive and

regularized diffusive Grad equations. For both the conventional and diffusive Navier-Stokes equations, the cross-stress component S_{xy} and normal heat flux component q_x were computed from the corresponding Newton and Fourier laws in (5.14). We do not show that diagonal components of the stress S_{xx} and S_{yy} , since they are quite small (about two orders of magnitude smaller than the cross-stress S_{xy} , and roughly four orders of magnitude smaller than the temperature).

Just as for the argon simulations above, observe that the results from the Navier-Stokes and Grad closures tend to match the boundary conditions for S_{xy} and q_x computed by the original DS1V routines, while the DSMC output of S_{xy} and q_x inside the domain (which was implemented by us in the DS1V program) is different by around 10%.

In Figure 6 we show the parallel component q_y of the heat flux for the DSMC simulation, as well as for the both conventional and regularized diffusive Grad approximations. Just as above for argon, observe that both Grad approximations capture the parallel heat flux qualitatively well, with some quantitative discrepancies.

7. THE COUETTE FLOW WITH REDUCED VISCOSITY AND SCALED DIFFUSIVITY NEAR WALLS

Assuming that all components v of the multi-particle velocity vector V from Sections 2 and 3 are statistically identical, and that their average values are zeros, observe that the scaled mass diffusivity D_α can be approximated, from (3.36) and (4.12), by the time autocorrelation function

$$(7.1) \quad D_\alpha = \alpha D = \alpha \tau_0 \rho \theta \approx \alpha \int_0^\infty \langle v(0)v(s) \rangle_f ds,$$

if we assume that f is sufficiently close to the statistical equilibrium. Above, the autocorrelation function $\langle v(0)v(s) \rangle_f$ is the average over all possible realizations originating from the initial states $v(0)$, while the initial states $v(0)$ are distributed according to f . At the same time, it is known that the viscosity μ of a gas is given by a similar time correlation function (see, for example, [18]).

As we can see, both the viscosity and scaled mass diffusivity depend on the ability of a gas particle to “forget” about its past states due to its chaotic motion. When the estimates of the viscosity and diffusivity are made, it is naturally assumed that the motion of the particle is uninhibited by external effects (such as the walls), and that it can permeate equally well in all directions.

However, if a wall is situated sufficiently close to the starting location of a particle (that is, within a few free mean paths), then, clearly, the particle will be prevented from permeating too far in the direction of the wall. Moreover, the fact that the particle is more likely to reverse its velocity as a result of the interaction with a wall, rather than the interaction with another particle, should cause more self-cancellations in the time autocorrelation integral above in (7.1), as well as in the viscosity time autocorrelation function in [18], which, apparently, should lead to the effective decrease in both viscosity and mass diffusivity in the immediate vicinity of the wall. The same conclusion follows from the common sense of the physics: taking into account that the diffusion coefficient indicates how rapidly a gas particle drifts away from its starting location on average as

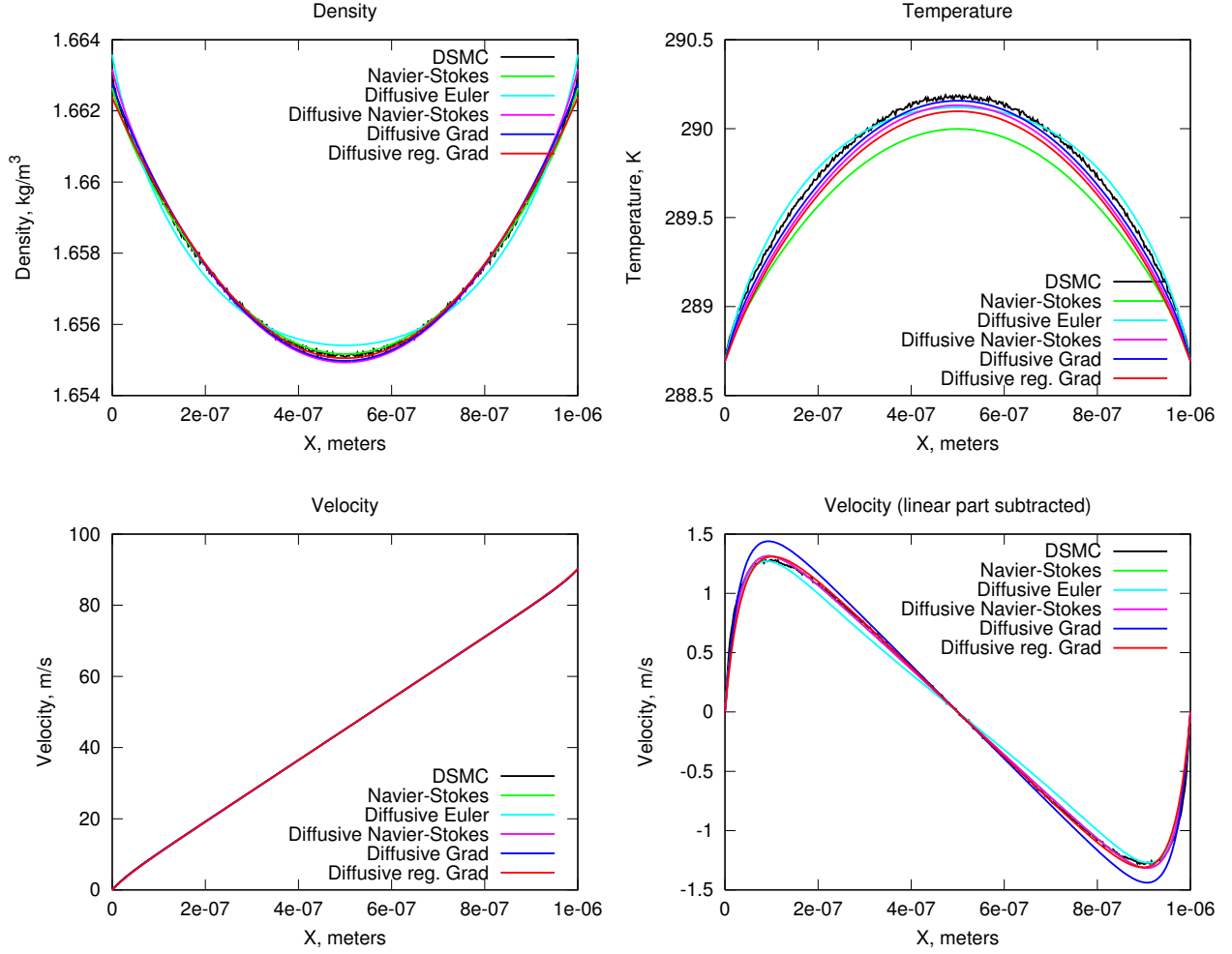


FIGURE 7. The density, velocity and temperature of the Couette flow for argon with near-wall reduction of viscosity and scaled diffusivity.

a result of collisions, observe that a nearby wall limits the possible drift outcomes, and must, therefore, on average decrease the rate of particle displacement and its diffusivity.

It might be possible to estimate the effect of a nearby wall on the autocorrelation integral in (7.1) rigorously under suitable assumptions on the trajectory of a particle and reflective properties of the wall, which will be the subject of future work. Here, however, for simplicity we instead suggest the following empirical scaling of both the viscosity and mass diffusivity near a wall:

$$(7.2) \quad \mu^{\text{near wall}} = \beta\mu, \quad D_{\alpha}^{\text{near wall}} = \beta D_{\alpha},$$

where the empirical scaling factor β , common for both μ and D_{α} , is given by

$$(7.3) \quad \beta(x) = (\beta_1 - 1)e^{-x/\beta_0} + 1,$$

where x is the distance to the wall, and β_0 and β_1 are constants, with $\beta_0 \sim$ mean free path, and $0 < \beta_1 < 1$. As we can see, the scaling $\beta(x)$ is defined such that it equals β_1

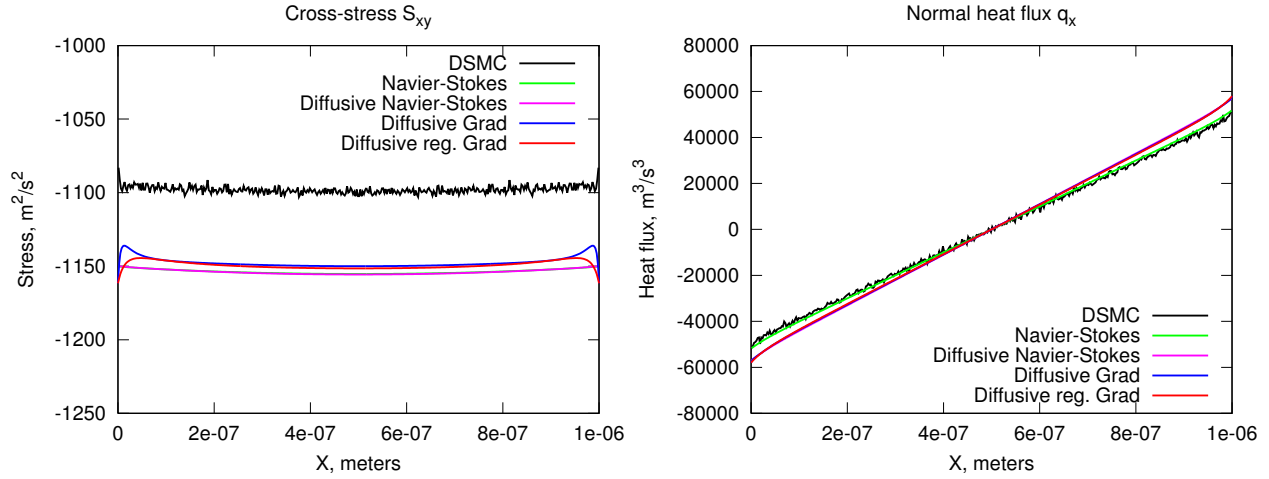


FIGURE 8. The stress and heat flux for the Couette flow for argon with near-wall reduction of viscosity and scaled diffusivity.

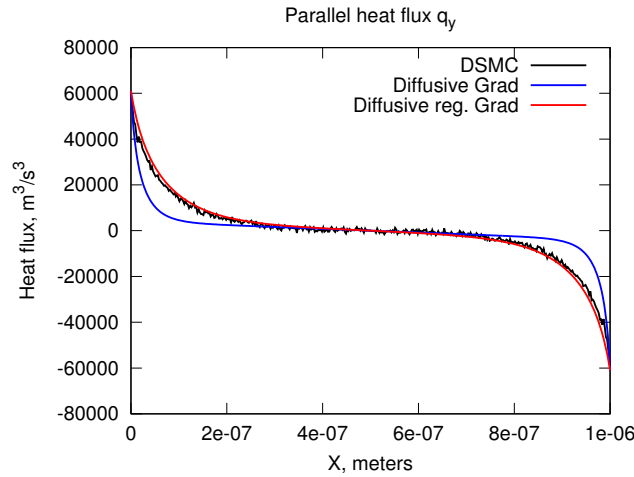


FIGURE 9. The parallel heat flux for the Couette flow for argon with near-wall reduction of viscosity and scaled diffusivity.

at the wall (that is, where $x = 0$), and approaches 1 exponentially rapidly away from the wall. We specify the parameters β_0 and β_1 empirically below.

7.1. The Couette flow with near-wall reduction of viscosity and scaled diffusivity for argon. For argon, we empirically set $\beta_0 = 4 \cdot 10^{-8}$ meters (which is of the same order as the mean free path at normal conditions) and $\beta_1 = 0.6$, while keeping all other parameters the same as above in Section 6. The results of the numerical simulations with reduced viscosity and scaled mass diffusivity are shown in Figures 7, 8 and 9. Observe that while the density and temperature on Figure 7 are largely unchanged, the velocity profiles on the same Figure now exhibit the full-fledged Knudsen boundary layers for all tested closures of the Boltzmann equation, from the diffusive Euler equations to both the diffusive and regularized diffusive the Grad equations. For the cross-stress S_{xy} and

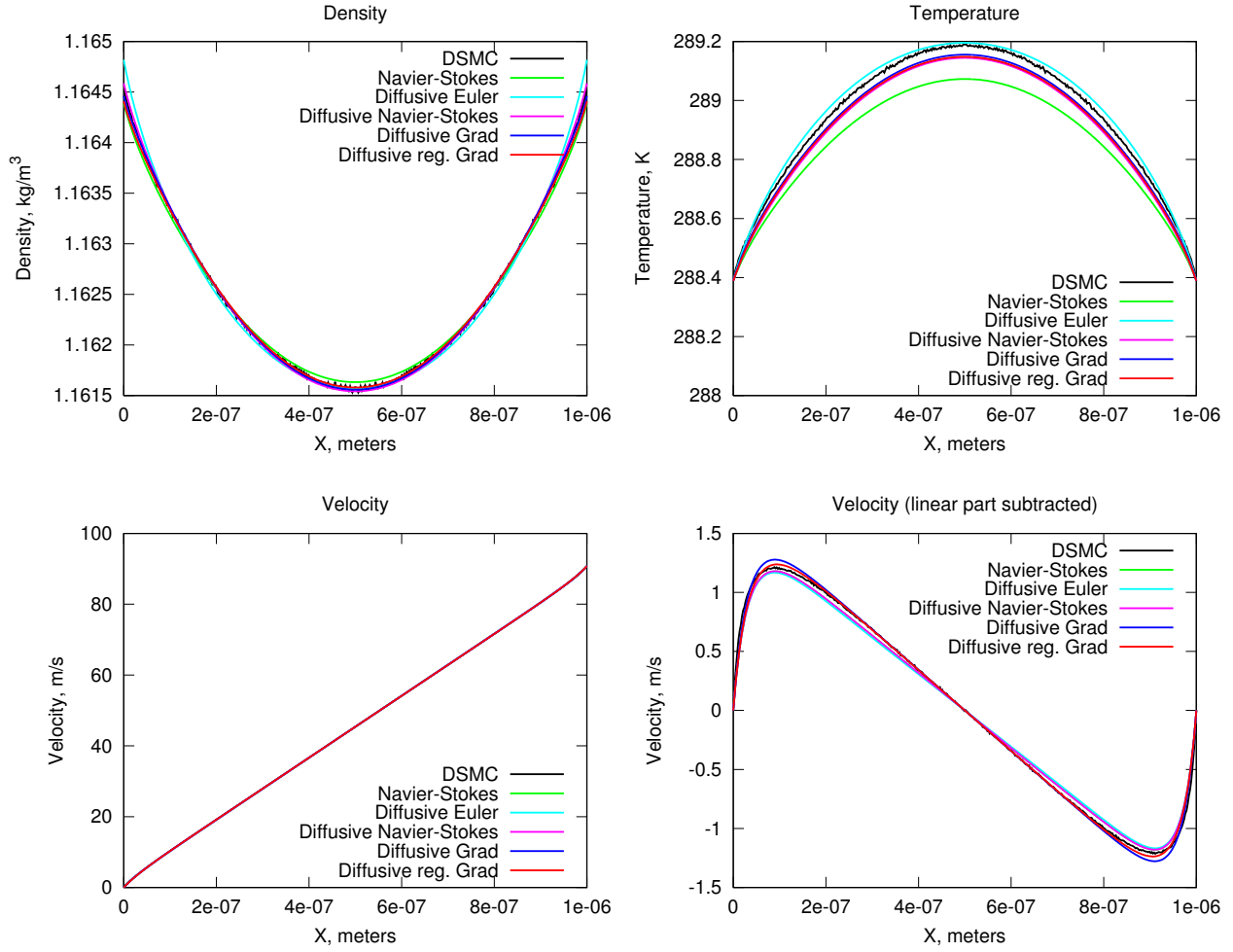


FIGURE 10. The density, velocity and temperature of the Couette flow for nitrogen with near-wall reduction of viscosity and scaled diffusivity.

normal heat flux q_x , we can see on Figure 8 that the results are not much different from those for unadjusted viscosity and scaled mass diffusivity above in Section 6, although there appears to be some minor improvement in capturing the cross-stress S_{xy} . What is surprising, is that the parallel heat flux q_y (Figure 9) is now captured by the diffusive regularized Grad equations quite precisely, unlike what was observed above in Section 6. Generally, it looks like the regularized diffusive Grad closure with the wall-adjusted viscosity is best for capturing both low- and high-order moments at the same time.

7.2. The Couette flow with near-wall reduction of viscosity and scaled diffusivity for nitrogen. For nitrogen, we set $\beta_0 = 3.75 \cdot 10^{-8}$ meters to roughly preserve the ratio between the free mean paths of nitrogen and argon at identical conditions, while empirically setting $\beta_1 = 0.62$ and keeping all other parameters the same as above in Section 6. The results of the numerical simulations with reduced viscosity and scaled mass diffusivity are shown in Figures 10, 11 and 12, and show essentially the same improvements as those above for argon. Observe that while the density and temperature are largely

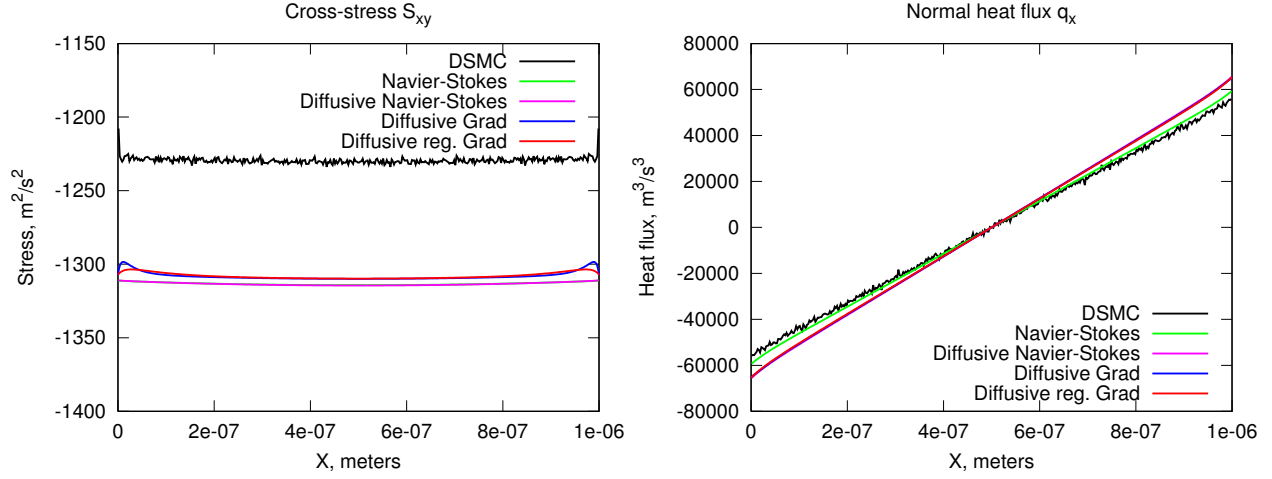


FIGURE 11. The stress and heat flux for the Couette flow for nitrogen with near-wall reduction of viscosity and scaled diffusivity.

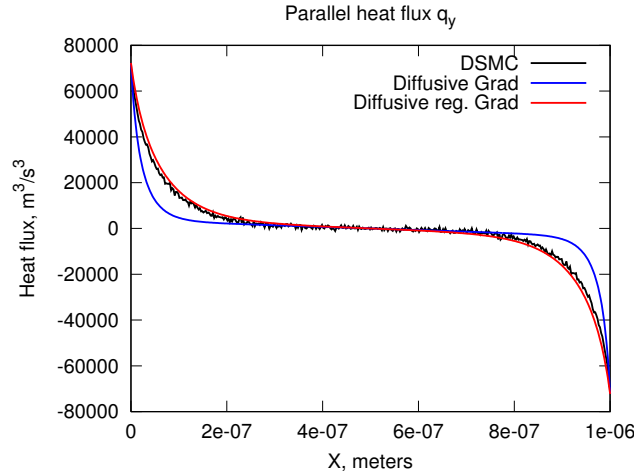


FIGURE 12. The parallel heat flux for the Couette flow for nitrogen with near-wall reduction of viscosity and scaled diffusivity.

unchanged, the velocity profiles now exhibit Knudsen-like boundary layers for all tested closures of the Boltzmann equation, from the diffusive Euler equations to the Grad equations (Figure 10). For the cross-stress S_{xy} and normal heat flux q_x , we can see on Figure 11 that, similar to the simulations with argon, the results are not much different from those for unadjusted viscosity and scaled mass diffusivity above in Section 6, although there appears to be some minor improvement in capturing the cross-stress S_{xy} . Just as for argon above, here the parallel heat flux q_y (Figure 12) is now captured by the regularized Grad equations very precisely, unlike what was observed in Section 6. Again, it looks like the regularized diffusive Grad closure with the wall-adjusted viscosity captures both low- and high-order moments at the same time better than any other closure, studied here.

8. SUMMARY

In this work we develop a spatially diffusive analog of the Boltzmann equation, based on the assumption of missed collisions in the model of the particle velocity process. For that, we first re-formulate the particle collision process as a random jump process, and show that, under suitable assumptions, the random jump model leads to the Boltzmann equation. Next, we apply the standard multiscale expansion formalism to the random jump model and compute the long-term homogenization dynamics for the coordinate of a particle. We model the effect of missed collisions via the appropriately scaled long-term homogenization process, which leads to the Boltzmann equation with an additional spatial diffusion term. We then obtain the hierarchy of the moment equations from the Boltzmann equation in a standard way, and carry out a computational study of the diffusive Euler, Navier-Stokes and Grad closures of the moment equations in a simple Couette flow setting with argon and nitrogen. We compare the results with the Direct Simulation Monte Carlo computations, and with the results produced by the conventional Navier-Stokes equations. We find that the diffusive Euler equations, and both the conventional and diffusive Navier-Stokes equations behave in a similar manner, producing rather accurate results for the density and temperature, but failing in capturing the Knudsen boundary layers in velocity. The diffusive and regularized diffusive Grad equations, on the other hand, produce the weak Knudsen-like velocity boundary layers, in addition to accurately capturing the density and temperature profiles.

Additionally, via a simple physics reasoning, we argue that both the viscosity and mass diffusivity must decrease in the vicinity of a wall. Using an empirical factor which reduces both the viscosity and scaled mass diffusivity near walls, we discover that all studied moment closures, from the diffusive Euler equations to both the diffusive and regularized diffusive Grad equations, develop the full-fledged Knudsen velocity boundary layers, closely matching the DSMC computations. Additionally, the component of the heat flux parallel to the flow (which is found to be of the same order of magnitude as the normal heat flux component) is captured quite well by the diffusive regularized Grad equations in the simulations with the near-wall reduction of the viscosity and scaled mass diffusivity. It would be interesting to check if any systematic quantitative theory for the value of the scaled mass diffusivity coefficient can be developed beyond the empirical approach adopted here.

For the future study, the natural step forward is to investigate the behavior of the new equations in capillary gas flows under normal conditions, as well as rarefied gas flows, in more advanced spatial configurations. One of the strong points of the new equations is that they combine the ability to model the flows of polyatomic gases (which are ubiquitous in nature) with the higher-order Grad closure, since, to our knowledge, thus far the Grad closure dynamics, where used, were confined to the monatomic set-up.

From the kinetic theory perspective, an interesting problem is to estimate the effect of the missed collisions onto the mass diffusion and viscosity coefficients, at least for some simple form of the collision kernel in the Lévy measure of the random jump process. In particular, common sense suggests that more missed collisions should statistically decrease the collision damping effect, and, therefore, increase the viscosity (since the latter enters the denominator of the collision damping). At the same time, the mass diffusion

should also increase in response to the stronger effect of missed collisions, since it compensates for those in a statistical manner via the long-term homogenization dynamics correction. Establishing the connection between the mass diffusion and viscosity in the form of the corresponding Schmidt number, depending on the fraction of the missed collisions, appears to be an important topic.

Also, it is interesting to see if the new equations can be used for modeling strongly turbulent flows, in particular, in the large scale atmospheric circulation. The assumption of imperfection in the particle collision process and subsequent coarse-graining via the homogenization dynamics is similar to what is done in the applications of turbulence, except that in the latter case the coarse-graining is applied to the Navier-Stokes equations in the form of the Reynolds averaging. It is likely that the major benefits of the diffusive and regularized diffusive Grad approximations should manifest in situations where the heat fluxes are important, as we observed that the Grad closures demonstrate the ability of capturing both normal and parallel heat fluxes (unlike the Navier-Stokes closures, which can only capture the normal heat flux in the studied set-up). An attractive feature of both the diffusive and regularized diffusive Grad closures is that the diffusive Grad equations allow to prescribe the stress and heat flux at the boundaries explicitly, which could lead to a more detailed model of the energy exchange between the atmosphere and the surface.

Acknowledgment. The author thanks Ibrahim Fatkullin for interesting discussions. The work was supported by the Office of Naval Research grant N00014-15-1-2036.

REFERENCES

- [1] D. Applebaum. *Lévy Processes and Stochastic Calculus*. Number 116 in Cambridge Studies in Advanced Mathematics. Cambridge University Press, 2nd edition, 2009.
- [2] D. Applebaum and A. Estrade. Isotropic Lévy processes on Riemannian manifolds. *Ann. Prob.*, 28(1):166–184, 2000.
- [3] L. Arnold, P. Imkeller, and Y. Wu. Reduction of deterministic coupled atmosphere-ocean models to stochastic ocean models: A numerical case study of the Lorenz-Maas system. *Dyn. Syst.*, 18(4):295–350, 2003.
- [4] G.K. Batchelor. *An Introduction to Fluid Dynamics*. Cambridge University Press, New York, 2000.
- [5] G.A. Bird. *Molecular Gas Dynamics and the Direct Simulation of Gas Flows*. Clarendon, Oxford, 1994.
- [6] H. Brenner. Kinematics of volume transport. *Physica A*, 349:11–59, 2005.
- [7] H. Brenner. Navier-Stokes revisited. *Physica A*, 349:60–132, 2005.
- [8] H. Brenner. Fluid mechanics revisited. *Physica A*, 370:190–224, 2006.
- [9] C. Cercignani. *Theory and Application of the Boltzmann Equation*. Elsevier Science, New York, 1975.
- [10] C. Cercignani. The Boltzmann equation and its applications. In *Applied Mathematical Sciences*, volume 67. Springer, New York, 1988.
- [11] C. Cercignani. Rarefied gas dynamics: From basic concepts to actual calculations. In *Cambridge Texts in Applied Mathematics*. Cambridge University Press, Cambridge, UK, 2000.
- [12] C. Cercignani, R. Illner, and M. Pulvirenti. The mathematical theory of dilute gases. In *Applied Mathematical Sciences*, volume 106. Springer-Verlag, 1994.
- [13] S. Chapman and T.G. Cowling. *The Mathematical Theory of Non-Uniform Gases*. Cambridge Mathematical Library. Cambridge University Press, 3rd edition, 1991.
- [14] S.K. Dadzie and J.M. Reese. Spatial stochasticity and non-continuum effects in gas flows. *Phys. Lett. A*, 376:967–972, 2012.

- [15] N. Dongari, R. Sambasivam, and F. Durst. Extended Navier-Stokes equations and treatments of micro-channel gas flows. *J. Fluid Sci. Tech.*, 4(2):454–467, 2009.
- [16] S. Duhr and D. Braun. Why molecules move along a temperature gradient. *Proc. Natl. Acad. Sci.*, 103(52):19678–19682, 2006.
- [17] F. Durst, J. Gomes, and R. Sambasivam. Thermofluidynamics: Do we solve the right kind of equations? In *Proceedings of the International Symposium on Turbulence, Heat and Mass Transfer*, pages 3–18, Dubrovnik, Croatia, 2006.
- [18] D. Evans and G. Morriss. Transient-time-correlation functions and the rheology of fluids. *Phys. Rev. A*, 38:4142–4148, 1988.
- [19] I.I. Gikhman and A.V. Skorokhod. *Introduction to the Theory of Random Processes*. Courier Dover Publications, 1969.
- [20] F. Golse. *Evolutionary Equations*, volume 2 of *Handbook of Differential Equations*, chapter The Boltzmann Equation and its Hydrodynamic Limits. Elsevier, 2006.
- [21] H. Grad. On the kinetic theory of rarefied gases. *Comm. Pure. Appl. Math.*, 2(4):331–407, 1949.
- [22] H. Grad. Principles of the kinetic theory of gases. In S. Flügge, editor, *Handbuch der Physik*, volume 12. Springer, Berlin, 1958.
- [23] M. Kac. Probability and related topics in physical sciences. In *Lectures in Applied Mathematics Series*, volume 1a. American Mathematical Society, 1957.
- [24] Y. Kifer. L^2 diffusion approximation for slow motion in averaging. *Stoch. Dyn.*, 3(2):213–246, 2003.
- [25] E.W. Lemmon and R.T. Jacobsen. Viscosity and thermal conductivity equations for nitrogen, oxygen, argon, and air. *Int. J. Thermophys.*, 25(1), 2004.
- [26] C.D. Levermore. Moment closure hierarchies for kinetic theories. *J. Stat. Phys.*, 83:1021–1065, 1996.
- [27] F. Mallinger. Generalization of the Grad theory to polyatomic gases. Research Report 3581, Institut National de Recherche en Informatique et en Automatique, 1998. E-print: INRIA-00073100.
- [28] A.S. Monin and A.M. Yaglom. *Statistical Fluid Mechanics, Volume 1: Mechanics of Turbulence*. MIT Press, 1971.
- [29] A.S. Monin and A.M. Yaglom. *Statistical Fluid Mechanics, Volume 2: Mechanics of Turbulence*. MIT Press, 1975.
- [30] B. Øksendal. *Stochastic Differential Equations: An Introduction with Applications*. Universitext. Springer, 6th edition, 2010.
- [31] G. Pavliotis and A. Stuart. *Multiscale Methods: Averaging and Homogenization*. Springer, 2008.
- [32] H. Risken. *The Fokker-Planck Equation*. Springer-Verlag, New York, 2nd edition, 1989.
- [33] H. Struchtrup. Grad’s moment equations for microscale flows. *AIP Conf. Proc.*, 663:792–799, 2003.
- [34] H. Struchtrup and M. Torrilhon. Regularization of Grad’s 13-moment equations: Derivation and linear analysis. *Phys. Fluids*, 15:2668–2680, 2003.
- [35] W. Sutherland. The viscosity of gases and molecular force. *Philos. Mag. S. 5*, 36(223):507–531, 1893.
- [36] M. Torrilhon and H. Struchtrup. Regularized 13-moment equations: Shock structure calculations and comparison to Burnett models. *J. Fluid Mech.*, 513:171–198, 2004.
- [37] E. Vanden-Eijnden. Numerical techniques for multiscale dynamical systems with stochastic effects. *Comm. Math. Sci.*, 1:385–391, 2003.